Middle-Late Quaternary Palaeoclimate Variability from Lake and Wetland Deposits in the Nefud Desert, Northern Arabia

Ash Parton[1,2,], Laine Clark-Balzan[3], Adrian G. Parker[1], Gareth W. Preston[1], Wing Wai Sung[4], Paul S. Breeze[5], Melanie J. Leng[6], Huw S. Groucutt[7,8], Tom S. White[9], Abdullah Alsharekh[10], Michael D. Petraglia[8]

[1] Department of Social Sciences, Oxford Brookes University, Headington Campus, Gipsy Lane, Oxford, OX3 0BP, United Kingdom

[2] Mansfield College, University of Oxford, Oxford, OX1 3TF, United Kingdom

[3] Albert-Ludwigs-Universitat Freiburg, Freiburg im Breisgau, Baden-Württemberg, Germany

[4] Department of Life Sciences, The Natural History Museum, Cromwell Road, London, SW7 5BD, United Kingdom

[5] Department of Geography, King's College London, Strand, London, WC2R 2LS, United Kingdom

[6] NERC Isotope Geosciences Laboratory, British Geological Survey, Nottingham, NG12 5GG, United Kingdom, and Centre for Environmental Geochemistry, University of Nottingham, Nottingham, NG7 2RD, United Kingdom

[7] School of Archaeology, Research Laboratory for Archaeology and the History of Art, University of Oxford, Oxford, OX1 2PG, United Kingdom

[8] Max Planck Institute for the Science of Human History, Kahlalsche Strasse 10, D-07745 Jena, Germany

[9] Department of Zoology, University of Cambridge, Downing Street, Cambridge, CB2 3EJ, UK

[10] Department of Archaeology, King Saud University, Riyadh, Saudi Arabia

Abstract

Records of former lake and wetland development in present day arid/hyper-arid environments provide an important source of information for palaeoclimatic and palaeoenvironmental studies. In Arabia, such records are typically confined to eccentricity-modulated insolation maxima, and are often spatially and temporally discontinuous. Here we present records from a single locality in Northern Arabia of wetter interludes during both global interglacial and glacial conditions, providing a unique opportunity to examine the nature of these events in a common setting. At Jubbah, in the southern Nefud Desert, lake and wetland deposits reveal the repeated formation of a water body within a large endorheic basin over the past ca. 360 kyr. Lake/wetland formation occurred during MIS 11/9, 7, 5, 3 and the early Holocene, assisted by local topographic controls, and spring recharge. Palaeoenvironmental and palaeoecological data reveal the existence of a large still water body formed during either MIS 11 or 9 (ca. 363 ka), and basin wide alluviation followed by lake formation during MIS 7 (ca. 212 ka). During MIS 5e (ca. 130 ka) a large freshwater lake occupied the basin, while during MIS 5a (ca. 80 ka) the basin contained a shallow wetland and freshwater lake complex. Lake/wetland formation also occurred during early MIS 3 (ca. 60 ka), at the Terminal Pleistocene-Holocene transition (ca. 12.5 ka), and the early-middle Holocene (ca. 9-6.5 ka). Phases of lake and wetland development coincided with human occupation of the basin during the Middle Palaeolithic, Epipalaeolithic and Neolithic periods, highlighting the significance of the region for early demographic change.

Keywords*: Pleistocene; Holocene; Paleoclimatology; Paleolimnology; Arabia; Stable isotopes; Luminescence Dating; Diatoms; Palaeolithic; Neolithic*

Corresponding Author: Ash Parton (aparton@brookes.ac.uk)

Department of Social Sciences, Oxford Brookes University, Headington Campus, Gipsy Lane, Oxford, OX3 0BP, United Kingdom

1. Introduction

Palaeoenvironmental records of lake and wetland development in desert regions provide an important means to better understand subtropical climate dynamics and the response of arid zones to climate change. Water bodies that form in these regions are sensitive to climatic changes (Battarbee, 2000), and constitute excellent records of hydrological responses to both regional and global climate variability (e.g. Trauth et al., 2003). In addition, arid regions such as the Saharo-Arabian desert belt have been the setting for major environmental changes throughout the course of human history, with large scale variations in water availability potentially driving the evolutionary and techno-cultural trajectories of human populations throughout the Pleistocene and Holocene periods (e.g. Staubwasser and Weiss, 2006; Trauth et al., 2007; Shea, 2008; Grove, 2012; Maslin et al., 2014; Groucutt et al., 2015a). Palaeoenvironmental and palaeoecological data derived from these records, therefore, also provide an important means to explore the connections between environmental change and past demographic variability.

Palaeolake development throughout Arabia is indicative of high amplitude oscillations in the dominant atmospheric systems that drive climate change across the peninsula. Situated within the subtropical Sahara-Arabian-Thar desert belt, the Arabian Peninsula lies at the interface of several complex and seasonally variable rain-bearing systems. Rainfall derived from the African and Indian Ocean monsoons, Mediterranean cyclones and Red Sea synoptic troughs, has contributed to large-scale hydrodynamic changes during the Pleistocene and Holocene periods (e.g. Engel et al., 2011; Fleitmann et al., 2011; Rosenberg et al., 2013; Parton et al., 2015a; 2015b; Preston et al., 2015). These include the widespread activation of major drainage systems, lake and wetland development, groundwater and aquifer recharge, speleothem and spring formation, and alluvial fan activation. Precipitation increases have also been accompanied by pervasive vegetative development and an associated increase in landscape stability. While our understanding of when and to what extent rainfall from each of these systems drove such changes remains fairly limited, palaeoenvironmental reconstructions from palaeolake and palaeowetland records have been used to develop a broad framework for establishing long-term, orbital-scale climate variability across the region.

Lacustrine and palustrine carbonates from the deserts of the Nefud, Rub' al Khali (Empty Quarter) and Wahiba (e.g. Radies et al., 2005; Parker et al., 2006; Rosenberg et al., 2011; 2013; Engel et al., 2011; Matter et al., 2015; Groucutt et al., 2015b; Preston et al., 2015), predominantly comprise relatively thin sequences (i.e. 1-3 m) of interstratified calcareous silts, sands and marls, relating to key pluvial periods such as MIS 5e (ca. 130-120 ka), 5c (ca. 105-95 ka), 5a (ca. 85-75 ka) and the early-mid Holocene period (ca. 11-6 ka). With the exception of a few records dated to early MIS 3 (e.g. Parton et al., 2013; Hoffmann et al., 2015; Matter et al., 2015; Jennings et al., 2016), lake and wetland formation overwhelmingly coincides with eccentricity-modulated insolation maxima. However, few records display evidence of repeated interglacial lake formation within the same basin, while none provide records of markedly wetter conditions during both glacial and interglacial periods.

The absence of continuity in Arabian lake records through glacial-interglacial cycles, and/or their lack of sensitivity to 'weaker' pluvials recently identified in fluvial-alluvial archives (Parton et al., 2015a), is likely determined by a combination of specific climatic and geomorphological controls. In the first instance, the predominance of high potential evaporative losses in Arabia (up to 3000 mm yr^{-1}) is such that precipitation must increase dramatically for substantial water bodies to form. This has typically occurred during interglacials. Indeed, Pleistocene-Holocene lake formation across Arabia corresponds closely with speleothem growth, which has occurred predominantly during interglacials (e.g. Fleitmann et al., 2003; 2011). For wetter periods that occur during drier global glacial conditions, such as the brief wet phase at the onset of MIS 3 (ca. 60-55 ka), high levels of evaporation combined with generally low rainfall levels may have been insufficient for significant lake formation or speleothem growth. This situation would also be exacerbated by the nature of rainfall across the peninsula, which would have likely comprised seasonally regulated high magnitude storm events.

Secondly, geomorphological settings exert significant control over both water body formation and archive preservation in dryland lakes. In some arid basins where the primary source of inflow is from the continuous discharge of allogenic rivers in more humid climatic zones, large perennial freshwater lakes may form. In Arabia, however, the major drainage systems that feed large basins such as Mundafan in the southern Rub' al-Khali and Tayma in northwest Arabia (Fig. 1), lie broadly within the same arid climatic belt, with only relatively minor (~150 mm) differences in annual rainfall between the basins and their montane headwaters. In addition, basin morphology plays a critical role in determining the permanency of a lentic water body through the provision of accommodation space. Palaeolake deposits in Arabia are mostly situated within shallow endorheic and/or deflationary basins. These may be interdunal depressions (e.g. Whitney et al., 1983; Parker et al., 2004; 2006; Radies et al., 2005; Rosenberg et al., 2013; Preston et al., 2015) or spatially extensive but flat depressions in which topographic depth is insufficient to enable water retention during periods of higher evaporation (e.g. McClure, 1976; Rosenberg et al., 2011a; Engel et al., 2011; Groucutt et al., 2015b). Similarly, there is a general paucity of lacustrine records that preserve more than one or two lake expansion phases within the same depression. As such, in order for lentic water body formation to persist beyond peak wet periods in Arabia, a unique set of geomorphic controls need to be in place to overcome high evaporative losses (e.g. Parton et al., 2013). Given these issues and the seasonality of the climate, all lake and wetland records from Arabia should be expected to reflect astatic water levels with one or more major evaporitic phases.

Here we present for the first time, a unique record of repeated long-term lake and wetland development spanning multiple interglacials from a large basin within the Nefud Desert, Northern Saudi Arabia. These comprise two ~9 m, one ~4 m and one ~2 m thick sequences composed of interstratified clays, marls, diatomites, silts, gypsum and sands. Multiproxy analyses have in turn revealed a detailed record of hydroclimatic change during the Middle-Late Pleistocene and Early Holocene periods. Our findings indicate the repeated development of an extensive water body over the past ca. 360 kyr during both global glacial and interglacial periods, due to favourable geomorphic controls and shallow groundwater. In addition, lake/wetland development is seen to correspond with the repeated hominin/human occupation of the region.

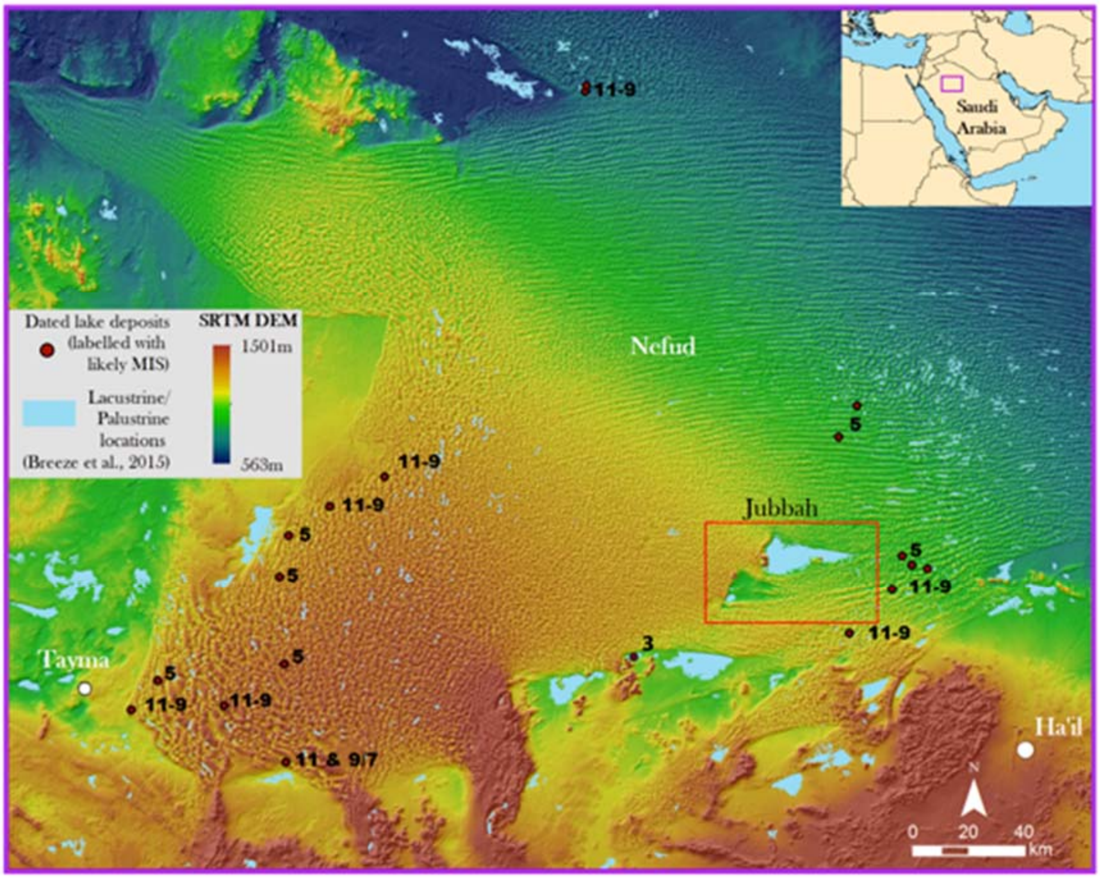

Figure 1: Map showing location of the Jubbah basin within the Nefud, including estimated extent of lacustrine/palustrine deposits (Breeze et al., 2015), and location of dated Pleistocene lake deposits reported by Rosenberg et al. (2013) and Stimpson et al. (2016), giving corresponding Marine Isotope Stage of lake formation.

2. Background

2.1. Physical Setting

The Nefud Desert (Fig. 1) is situated within a depression that covers ~375,000 km^2 and dips gently to the northeast. The sand sea itself covers some 57,000 km^2 between Jawf and Ha'il regions, with an average elevation of ~900 m asl (Vincent, 2008). The desert sands have accumulated to a depth of up to ~100 m, and extend east to the ad-Dahna sand belt, through which they are linked to the Rub' al-Khali in the south. In the north and south, the Nefud is characterised by complex linear dune ridges oriented parallel to the prevailing wind, while central and western regions are predominantly composed of compound barchanoid dunes. The underlying depression is situated within the Interior Shelf; an outcrop of Palaeozoic to Lower Cretaceous detrital rocks that surround the Arabian Shield in a semi circle from Tabuk and the Widyan basin margin in the north, to the Wajid basin in the southeast. The major structural elements of the northern parts of the shelf comprise vast outcrops of Cambro-Ordovician sandstones, which dip gently towards the east-northeast, and occasionally outcrop from their covering of Quaternary sediments (Wagner, 2011).

Groundwater within the region is derived from the Saq aquifer, which extends across 375,00 km^2 in Saudi Arabia and Jordan (Alsharhan et al., 2001), forming the major aquifer for both countries. Groundwater occurs within the Saq under both confined and unconfined conditions, and flows east towards the Jubbah region under an average hydraulic gradient of 0.017 (Hussein et al., 1992; Barthélemy et al., 2007). While more saline at greater depth, groundwater within the aquifer is fresh and of good quality at the margin of sandstone outcrops, extending considerable distances from the areas beneath the overlying confining strata (Lloyd and Pim, 1990). Presently, aquifer recharge occurs through high intensity storms, and resulting in ~3-11 mm of recharge per year across the region (Fisk and Pim, 1985; UN-ESCWA and BGR, 2013). Runoff is minimal, however, infiltration of rainfall through the dunes may be significant. Within the region, annual rainfall of ~80 mm per year will produce approximately 20 mm of water recharge to local and shallow aquifers through the dunes (Dincer et al., 1974), allowing seepage into topographic depressions, facilitating vegetation growth and by extension, increasing landscape stability. During previous periods of substantially higher rainfall, infiltration through the dunes surrounding depressions would have been a major contributor to lake water recharge, while also extending the recharge phase beyond that of the rainy season.

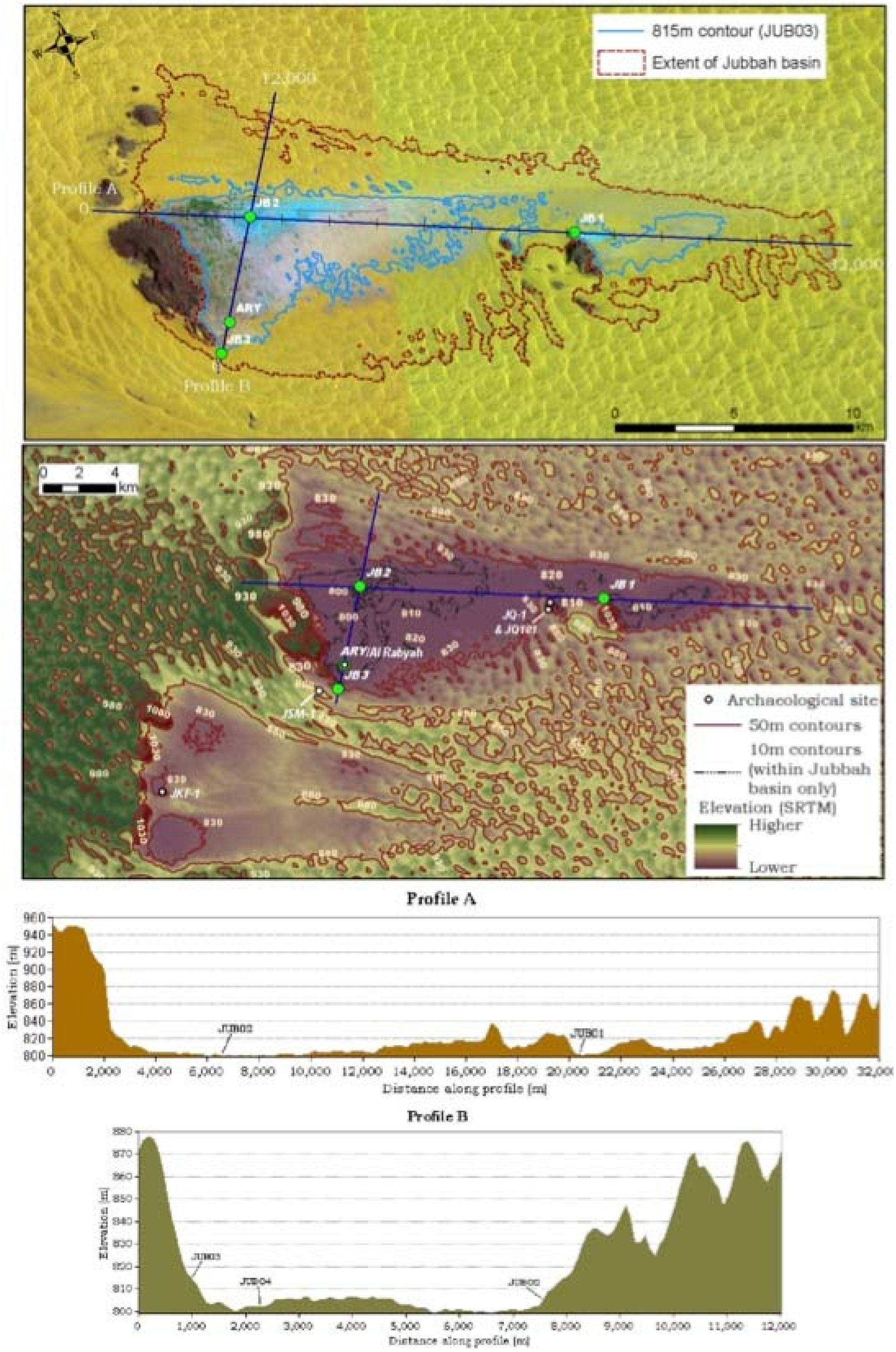

Figure 2: Figure showing map of the Jubbah basin and location of the four studied sections; (JB1-3 & ARY), and previously reported archaeological sites and palaeoenvironmental records (JQ-1 (Petraglia et al., 2012), JQ-101

(Crassard et al., 2013), JKF-1 (Groucutt et al., 2015c) and JSM-1 (Groucutt et al., 2017)).

2.2. The Jubbah Basin

The Jubbah basin is the largest endorheic depression in the south-central Nefud (Fig. 1 & 2). It lies approximately 80 km northwest of Hail, and ~50 km inside the southern border of the sand sea. The basin is situated at ~800 m asl and is bordered on its northern and southern sides by compound barchanoid dunes that extend up to 80 m above the basin floor. At the western margin of the basin, Jebel Umm Sanman rises to ~200 m above the basin, its presence sheltering the depression from the eastward transport and accumulation of aeolian sand. The overall maximum extent of the Jubbah depression is ~32 km (west-east) by ~12 km (north-south), covering a total area of ~177 km^2. This is defined by the areas facing downslope into the basin, the surrounding dune faces, and exposed surfaces underlying the dunes that form the basin floor. The latter accommodates two distinct basins within the 815 m contour range, which denotes the maximum elevation at which preserved lacustrine/wetland deposits are recorded within the basin. No preserved shoreline deposits were observed within the basin. This is likely due to the substantial urban and agricultural development that has taken place across the Jubbah basin, combined with burial by later phases of dune reactivation along the fringes of the depression. To the west, a larger basin directly sheltered by Jebel Umm Sanman is ~44 km^2. To the east, the smaller Jebel Ghawtah range rises to a height of 1082 m asl, and has similarly led to the development of a small deflationary basin approximately 7.8 km^2. Both ranges have Saq sandstone at their base and Tabuk sandstone near their summit (Bramkamp et al., 1963). Throughout the basin, groundwater lay near to the modern surface as recent as the late 19th Century (e.g. Blunt, 1881), with the town of Jubbah forming an oasis that has been repeatedly occupied over recent centuries and millennia (Jennings et al., 2014). Due to modern agricultural practices, however, water now lies at a depth of at least ~50m, with recent groundwater depletion models (Al Salamah et al., 2011) suggesting that drawdown may currently be as great as 1 m per year. At the eastern end of the basin, fossil spring outcrops are reported by Crassard et al. (2013), which represent areas of focused discharge of the Saq aquifer.

Pleistocene and Holocene lacustrine and palustrine records have been reported from the Jubbah region, often associated with archaeological assemblages (Fig. 2). Lower Palaeolithic assemblages have been identified at Jubbah and in other nearby basins, yet they currently lack precise chronological attribution (Shipton et al., 2014). Petraglia et al. (2011; 2012) describe a perched sequence of isolated palaeosols and lacustrine sediments at the site of Jebel Qattar-1 (Fig. 2) that are stratigraphically bounded by aeolian sediments and dated to MIS 5 and MIS 7, with both periods having associated Middle Palaeolithic archaeological material. The MIS 7 assemblage currently represents the earliest dated Middle Palaeolithic material from the Arabian Peninsula. The site of JSM-1, located just south of Jebel Umm Sanman (Fig. 2), produced a Middle Palaeolithic assemblage, which probably dates to late MIS 5 (Petraglia et al., 2012). A small lake is also reported from an adjacent basin at Jebel Katefeh (Petraglia et al., 2012; Groucutt et al., 2015c), which represents a phase of human occupation associated with Middle Palaeolithic technology. Reported ages from the site indicate a possible MIS 5a age (ca. 90-85 ka) for lake formation, however, a notable population of younger grains (ca. 50 ka) highlight the potential for an early MIS 3 age of the site. Indeed, hominin occupation of the Nefud during early MIS 3 (ca. 60-50 ka) is reported from the Al Marrat basin, which is located ~50 km southwest of Jubbah (Fig. 1) (Jennings et al., 2016). If the MIS 5 age estimates are correct, then the technological differences between JKF-1, JSM-1 and JQ-1, suggest considerable demographic and behavioural complexity within the Jubbah basin at this time (Scerri et al., 2015). Given recent interest in processes such as the dispersal of *Homo sapiens* out of Africa and admixture between *Homo sapiens* and Neanderthals, refining the chronology of archaeological and palaeoenvironmental sites at Jubbah remains a key task.

Evidence for Holocene-age lake formation within the Jubbah basin is reported by Crassard et al. (2013), who describe a small sequence of lacustrine silts featuring plant macrofossils and reed stems, indicative of shallow water conditions, dated to ca. 9-8 ka. It was argued by Crassard (2013) that the lithic assemblage at the adjacent JQ-101 archaeological site (Fig. 2), demonstrated similarities (particularly in arrowhead forms) with the Pre Pottery Neolithic, previously known from the Fertile Crescent. At the site of Al Rabyah (Fig. 2), Hilbert et al. (2014) report a sequence of palustrine-type sediments dated to ca. 6.5 ka, which reflect shallow but perennial and well-vegetated conditions, underlain by deposits indicative of deeper water conditions dated to at least ca. 12 ka. A lithic assemblage located in sandy sediments between these two phases of lake formation at Al Rabyah is similar to Epipalaeolithic assemblages known from the Levant, particularly those assigned to the Geometric Kebaran. Ostensibly the findings from the Nefud agree with the wider picture of lake formation across Arabia, with the timing of lake development corresponding to eccentricity-paced insolation maxima. These appear to have allowed cultural connections with the Levant to the north, but the precise form these interactions took remains unclear and a key topic for future research. The extent to which demographic and behavioural changes in the Holocene represent autochthonous developments, cultural diffusion, and population dispersal has been debated (see e.g. Guagnin et al., 2015), and a key area of resolution rests on the recovery of securely dated archaeological, palaeontological and palaeoenvironmental data from this region.

A report by Garrard et al. (1981) describes a ~26 m interstratified sequence comprising seven major sedimentary units composed of clays, carbonates and sands, which were deposited directly on top of the Saq sandstone. The lowermost units were ~12 m of clays, overlain by ~12 m of calcareous diatomaceous silts. The uppermost units described in the study were positioned on the banks of a shallow drainage runnel adjacent to Jebel Umm Sanman, located approximately 1.5 km west of the deep sequence described above. These comprised an interstratified sequence of sand, silt and diatomite dated by ^{14}C to 25,630±430 B.P., overlain by a palaeosol dated to 6,685±50 B.P. (Garrard et al., 1981). The findings presented here comprise the first detailed palaeoenvironmental and palaeoecological analysis of the deposits initially described by Garrard, along with a substantially revised and detailed chronology based on OSL and radiocarbon dating techniques (see Clark-Balzan et al., 2017 for further details of the chronology presented here). In addition, this study provides an important framework for the demographic changes reported in the aforementioned archaeological studies.

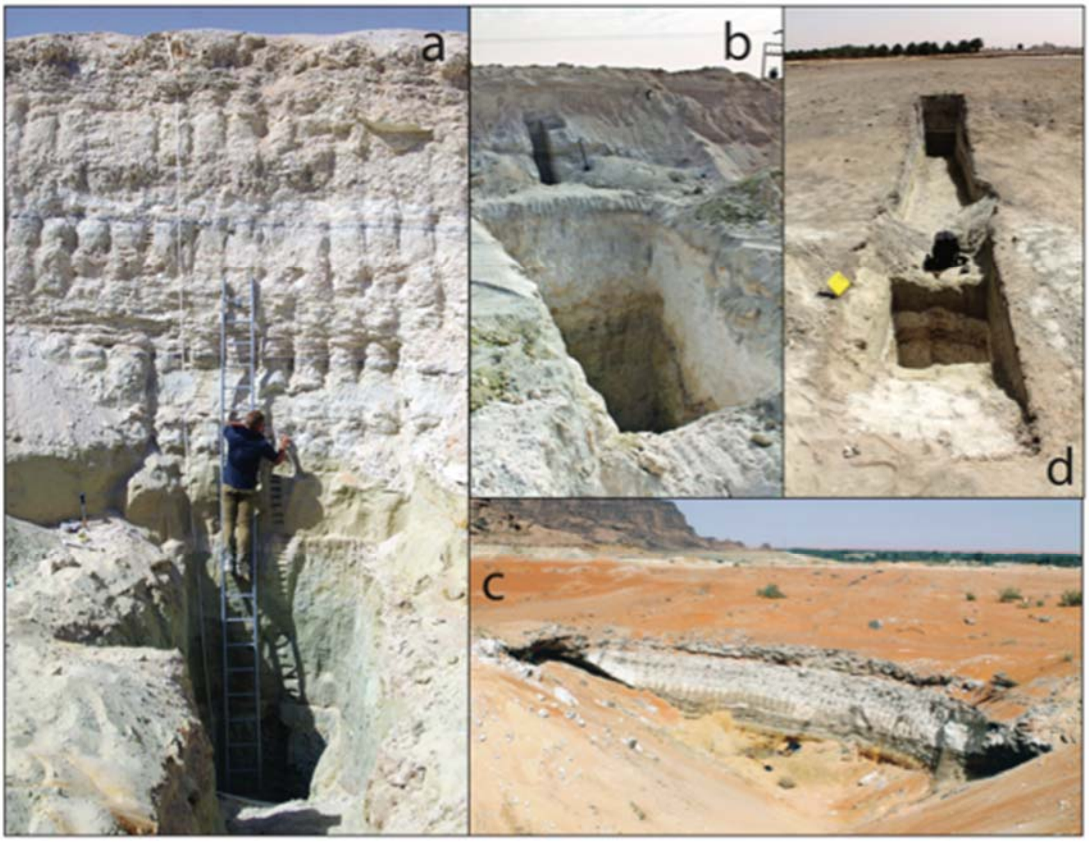

Figure 3: Photographs showing the excavated sections at JB1 (a), JB2 (b), JB3 (c) and Al Rabyah (ARY) (d).

3. Methods and Materials

Four sedimentary sequences comprising palaeolake and palaeowetland deposits were excavated within the Jubbah basin (Fig. 2 & 3). At the eastern end of the basin (28.020381 N, 41.095013 E), a sequence approximately 0.3 km from the base of Jebel Ghawtar (JB1) was excavated to a depth of 9.5 m. At the western end (28.020993 N, 40.955891 E), a sequence approximately 3 km from the base of Jebel Umm Sanman was excavated to a depth of 8.5 m (JB2). A third sequence (JB3), situated approximately 0.3 km from the base of Jebel Umm Sanman (27.974871 N, 40.925377 E) was excavated to a depth of 4 m. New data and an additional OSL age (Clark-Balzan et al., 2017) is also reported from a fourth sequence (Al-Rabyah - ARY), which is situated ~1 km north of JB3 and previously described by Hilbert et al. (2014). Samples were extracted from all sites for palaeoenvironmental/palaeoecological laboratory analyses. A more detailed multiproxy analysis was conducted at the deepest and most stratigraphically complex section, JB1.

Analyses of organic carbon (LOI_{org}) and carbonate content (LOI_{carb}) were conducted following the standard procedure described by Dean (1974) and Heiri et al. (2001). Environmental magnetic susceptibility measurements were determined following Dearing (1999). Samples for bulk (<63 mm fraction) inorganic carbonate isotope analysis ($^{18}O/^{16}O_{carb}$ and $^{13}C/^{12}C_{carb}$) of the JB1 sequence were prepared following standard off line vacuum extraction procedures (e.g. Lamb et al. 2000) and all measurements made using a VG Optima mass spectrometer. The stable isotope analyses were conducted at the NERC Isotope Geosciences Laboratory, Keyworth, Nottingham. Conductivity measurements were made using a Jenway Model 470 Conductivity Meter. For laser granulometry of the <2 mm sediment component, samples were disaggregated in de-ionised water with 5% sodium hexametaphosphate, and analysed using a Malvern Mastersizer 2000.

Samples for diatom analysis were prepared using the methods outlined by Renberg (1990). 30% H_2O_2 and 5% HCl were added to samples to digest organic material and remove calcium carbonate. After heating the samples were diluted with distilled water and stored in the refrigerator. The samples were rinsed daily and allowed to settle overnight for four days. The slides were air-dried at room temperature in a dust free environment prior to mounting with Naphrax diatom mountant. Diatom taxonomy followed Krammer and Lange-Bertalot (1986; 1988; 1991a; 1991b), Poulíčková, and Jahn (2007), Saros and Anderson (2015), and Nakov et al. (2015). Ideally 300 hundred valves should be enumerated for a representative sample; however, in certain circumstances, i.e. for samples with low abundances, a modified enumeration strategy can be used to enable fewer valves to be counted (Battarbee et al., 2001). Samples with fewer than 100 valves were omitted from subsequent analyses, as these do not provide a representative sample since most change in species occurs between 0 and 100 valves. Correspondence Analysis was used to examine the prevalent trends in the assemblage after Detrended Correspondence Analysis showed that the gradient length was greater than 1.5 SD units using the program CANOCO version 4.5 (Ter Braak and Prentice, 1988). Theorised zones of sedimentation and palaeoenvironmental change at the sites were derived from all palaeoenvironmental proxy data using the optimal sum of the squares partitioning with the program ZONE (Lotter and Juggins, 1991; *unpublished*). Statistically significant zones were deduced by comparison with the Broken Stick model using the program BSTICK version 1 (Bennet, 1996).

3.1 Chronology

Radiocarbon dating was attempted at JB1. Two charred plant fragments collected in the field (2.58 m, 2.65-2.68 m) and five bulk sediment samples from horizons determined to be rich in organic carbon (0.40-0.50 m, 0.85-0.90 m, 3.05-3.15 m, 3.40-3.50 m, 4.26-4.28 m) were submitted to the Oxford Radiocarbon Accelerator Unit (ORAU) (for protocols see Bronk Ramsey et al. (2002) and Bronk Ramsey et al. (2004)). Of these, only the unidentified plant fragment at 2.65-2.68 m could be dated after pretreatment. This sample was dated to 7925 ± 45 ^{14}C years BP, which is calibrated for a final age of 8980-8609 cal BP at the 95.4% range via the IntCal13 calibration curve (Reimer et al., 2013) using OxCal v4.2 (Bronk Ramsey, 2009). Factors that might have influenced the use of this radiocarbon date as an estimator for the depositional age of the surrounding sediment were considered (Clark-Balzan et al., 2017), including bioturbation, overestimation of age due to residence times before burial (affecting woody plants; see Oswald et al., 2005), underestimation due to inherited geological carbon (affecting submerged and emergent plants; see Marty and Myrbo, 2014) due to nearby carbonates and Saq aquifer waters (20,400 ± 500 ^{14}C years, Thatcher et al., 1961), and contamination by modern carbon. We consider that this sample provides a reliable depositional age.

A combined quartz OSL and feldspar post IR-IRSL (290 °C) (pIRIR$_{290}$) luminescence dating study was implemented for these sites. For full details of this project, see Clark-Balzan (2016) and Clark-Balzan et al. (2017); pertinent details are summarized here. Samples for luminescence dating were collected by hammering sections of plastic or metal tubing into the cleaned section face, after which these were capped. The full depth of the section was systematically sampled at a resolution of one sample per approximately every 0.50 m (JB1—JB3) or higher (ARY). Sand-rich layers were preferentially targeted, followed by carbonate-rich/gypsum-poor layers; highly gypsiferous units were sampled only if no other suitable unit was available near the chosen depth. Water content samples were also collected, and gamma spectrometer measurements were made on site for all samples except ARY-OSL4. Mineral extraction followed procedures given in Hilbert et al. (2014) for the quartz samples from ARY, and slightly altered procedures in Clark-Balzan (2016) and Clark-Balzan et al. (2017) designed to reduce the proportion of gypsum in the measured extracts. Quartz D_e's were measured via a blue-light OSL SAR protocol (Murray and Wintle, 2000; 2003) incorporating recycled, zero-dose, and IR depletion steps (Duller, 2003). Feldspar D_e's were measured via the pIRIR290 protocol (Thiel et al., 2011a, b), which also incorporates recycled and zero-dose steps. Supplemental experiments included a dose recovery (12 aliquots for D_e + 4 for bleaching residual) and fading characterization (Huntley and Lamothe, 2001; Auclair et al., 2003). Additionally, pIRIR290 D_e's were measured from 20 aliquots of a modern aeolian surface sample to check for an unbleachable residual, and IR_{50} and $pIRIR_{290}$ residuals were calculated by comparing feldspar and quartz D_e's from five ARY samples order to examine geological signal inheritance. DRAC (Durcan et al., 2015) was used to calculate dose rates: alpha (for unetched quartz and all feldspars), beta, and gamma (only ARY-OSL4) dose rates were calculated from elemental concentrations determined via ICP-MS.

The number of samples and the minerals measured for dating the sequences described here are summarized thus:

- Al Rabyah (ARY): two quartz ages (plus four from Hilbert et al., 2014), five feldspar ages for residual estimation
- JB1: one quartz, five quartz + feldspar, three feldspar; two additional elemental concentration samples
- JB2: six quartz, one feldspar; four additional elemental concentration samples
- JB3: three quartz, one quartz + feldspar

Luminescence D_e distributions, dose rate assessments, and age-depth relationships were thoroughly examined. Both quartz OSL and feldspar pIRIR290 protocols seem to provide accurate assessments of D_e, based on rejection criteria and D_e's and similar studies from the same region (for quartz) and a dose recovery experiment (feldspar). Quartz and feldspar ages, too, are congruent for multiple samples from JB1, though $pIRIR_{290}$ residuals are also apparent. Two samples dated via quartz are suspected to be partially bleached after inspection of D_e distributions based on overdispersion and skewness, while feldspar residuals calculated from ARY provide evidence for a non-systematic geological signal inheritance of up to ca. 50 Gy. We did not see any evidence for physical mixing of grains or, surprisingly, systematic underestimation of quartz D_e's due to saturation effects (cf. Groucutt et al., 2015b; Rosenberg et al., 2011a, b). Fading experiments for the feldspars showed only low levels of fading, which are expected to be laboratory artifacts. Examination of age-depth inversions, comparison of the radiocarbon age and bracketing OSL ages, uranium concentrations (up to 45.4 ppm), and thorium/uranium ratios, however, led to the conclusion that dose rates were overestimated for a number of samples from carbonate-rich levels. These samples are likely to suffer both from disequilibrium in radioisotope decay chains and post-depositional uranium enrichment via carbonate re-precipitation (Faure, 1986; Krbetschek et al., 1994; Olley et al., 1996; Dill, 2011). This is particularly a problem when dose rates are calculated from elemental concentrations as they have been in this study, due to the assumptions underlying the conversion factors (Guérin et al., 2011). No constraints on the timing of the uranium enrichment could be given; therefore the ages could not be modelled to account for this. Instead, all of the evidence was considered, and the ages shown in Table OSL1 were judged to be the most reliable based on the characterization of the units, the elemental concentrations, and the age-depth relationships.

Table 1: Reliable ages from the luminescence dating study of Clark-Balzan et al. (2017) for ARY, JB1, JB2, and JB3. Quartz luminescence measurements (excluding ARY-OSL4) were made upon unetched quartz (125-180 µm, 2 mm aliquot diameter); for ARY-OSL4, etched quartz (180-255 µm, 4 mm aliquot diameter) was used in order to be directly comparable with results from Hilbert et al. (2014). Feldspar pIRIR290 measurements are reported from 180-255 µm grains, 1 mm aliquot diameter. See text and Clark-Balzan et al. (2017) for further details. Note that the depth of OSL samples given for JB3 include 0.7 m of disturbed surface that are not shown in Figures 4 and 8.

Field Code	Lab Code	Depth (m)	Mineral	Measured (# aliquots)	Accepted (# aliquots)	Overdispersion (%)	D_e (Gy)	D_r (Gy ka^{-1})	Age (ka)
ARY-OSL4	X6141	0.45	Q	15	14	19.21 ± 4.00	9.22 ± 0.50	1.44 ± 0.05	6.4 ± 0.4
JB1-OSL5	X 6250	4.51	F	10	10	19.43 ± 6.79	357.06 ± 28.46	4.86 ± 0.23	73.4 ± 6.8
JB1-OSL8	X 6253	5.50	F	10	8	43.49 ± 11.9	302.45 ± 48.79	2.23 ± 0.16	135.8 ± 23.9
JB1-OSL13	X 6258	9.00	F	10	5	47.96 ± 18.18	889.16 ± 209.98	4.30 ± 0.20	206.6 ± 49.7
JB2-OSL1	X 6216	0.77	Q	18	12	14.43 ± 4.62	5.93 ± 0.32	0.69 ± 0.03	8.6 ± 0.6
JB2-OSL4	X 6219	3.94	Q	20	7	18.24 ± 6.62	9.78 ± 6.62	1.14 ± 0.05	8.6 ± 0.8
JB2-OSL14	X 6228	8.65	F	8	6	54.11 ± 16.17	844.81 ± 189.89	2.35 ± 0.16	359.4 ± 84.3
JB3-OSL1	X 6231	1.20	Q	18	14	52.18 ± 10.31	61.63 ± 8.79	1.10 ± 0.04	56.2 ± 8.3
JB3-OSL2	X 6232	1.67	Q	18	14	48.08 ± 9.90	55.00 ± 6.32	0.83 ± 0.03	66.3 ± 8.0
JB3-OSL3	X 6233	2.07	Q	18	10	62.22 ± 14.42	83.60 ± 16.75	0.83 ± 0.03	100.5 ± 20.5
JB3-OSL4	X 6234	2.50	Q	18	11	30.83 ± 7.77	94.98 ± 9.64	1.26 ± 0.05	75.3 ± 8.1

4. Results

Zonation of key depositional phases is shown along with multiproxy palaeoenvironmental and palaeoecological records in Figures 5-9. Due to insufficient carbonate material, isotope values were not obtained from units 1-6 at JB1. A total of 84 diatom species were identified at JB1, and only species with an abundance of over 12% (14 taxa) are shown. At ARY, a total of 76 diatom species were identified with an abundance of 7% (15 taxa) shown. A notable feature of the sequences at JB1 and JB2 is their depth (9.5 m and 8.5 m respectively) compared to those previously reported from Arabia, which generally range from 0.5-2.0 m. In addition, unlike those previously reported from the Nefud, the sequences display a highly complex stratigraphy featuring interstratified clays, gravels, marls, gypsum, diatomite, silts and sands.

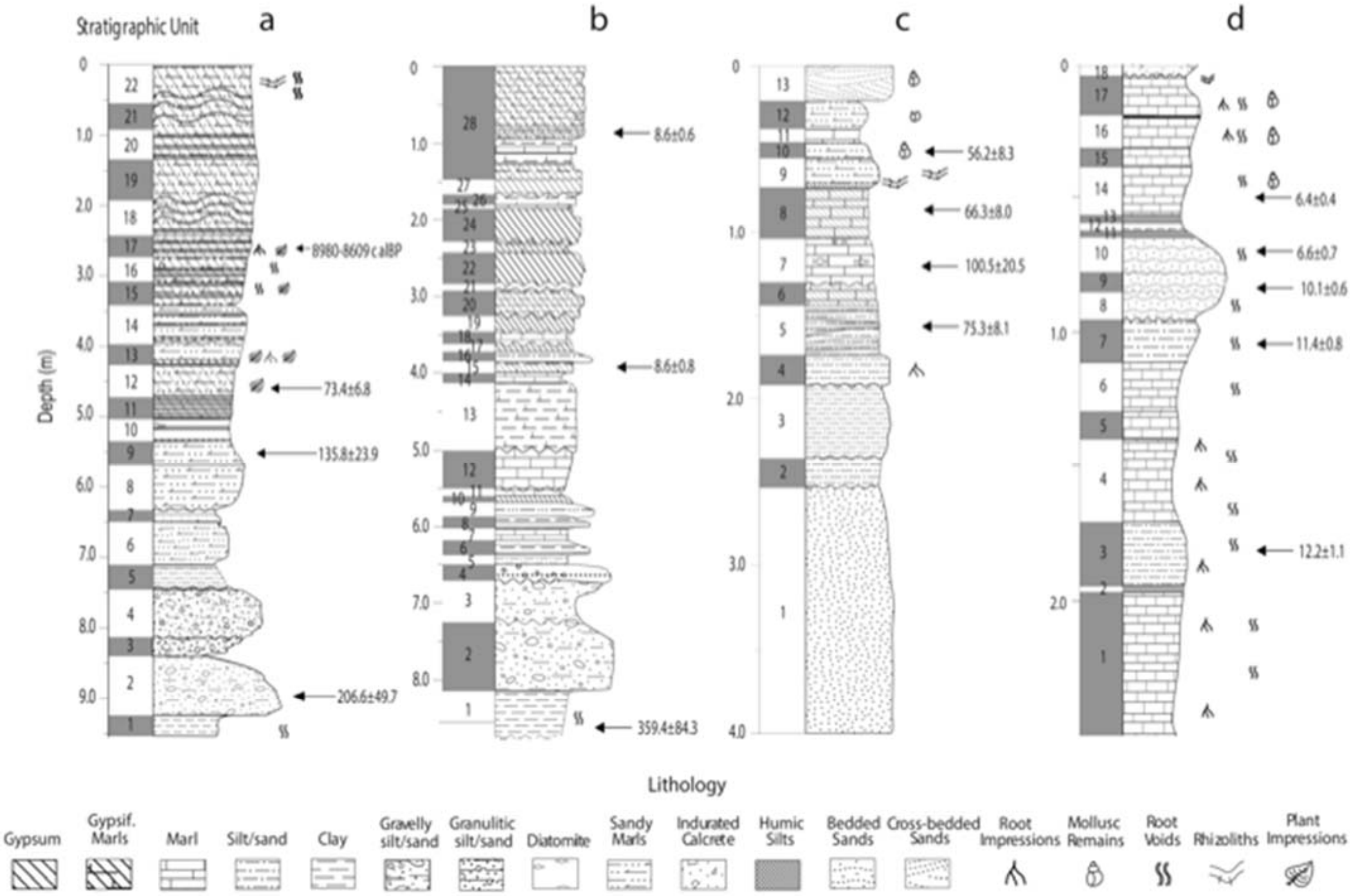

Figure 4: Stratigraphy of sequences JB1 (a), JB2 (b), JB3 (c) and ARY (d), showing reliable ages derived from each section. Note, for illustrative purposes, section depths do not utilise the same scale.

4.1. Middle and Late Pleistocene Proxy Records

The chronology for each sequence was predominantly constructed from ages derived directly from waterlain sediments, and are therefore representative of wetter periods. Phases of Middle and Late Pleistocene sedimentation within the Jubbah basin are reported from JB1, JB2 and JB3, the oldest of which (359.4±84.3 ka) is recorded at JB2 (JB2-OSL14). Due to substantial error ranges on this date, this phase may be attributable to increased rainfall during either MIS 9 (ca. 337-300 ka) or MIS 11 (424-

374 ka). While this phase of lake formation is most likely indicative of one of these wet phases, the overlapping error range with both MIS 11 and 9 currently prohibits a firm assignment to either period. The unit is free from large gravel clast inclusions, interbedding or bioturbation, indicating undisturbed still water deposition and the dissolution of underlying sandstone bedrock material. Notably similar sedimentary characteristics are observed at the base of JB1 (Unit 1), possibly reflecting contemporaneous formation. At JB1, lower gravelly silt/sands are likely to be older than 206.6 ± 49.7 ka (JB1-OSL13), though a minimum age of 151.9 ± 36.0 ka calculated due to the existence of an outlying, younger aliquot cannot be entirely ruled out (see Clark-Balzan et al., 2017). Given these ages and the corresponding errors, we suggest that this phase of sedimentation corresponds with increased regional rainfall during MIS 7. This depositional phase is characterised by the mobilisation and deposition of weathered material from the adjacent Jebel Ghawtar. As before, similar gravelly sediments are observed overlying the lowermost clayey deposits at JB2, which again may reflect the contemporaneous deposition of these facies across the wider basin. A lack of reliable ages from this unit at JB2, however, prevents confirmation of this. In both sequences a sharp, uniform bounding surface with no evidence of scouring separates gravel and clay units, which likely reflects a depositional hiatus between the units.

At both JB1 and JB2, gravelly/granulitic sediments gradually progress into a sequence of interbedded silt-sands and finely laminated marls. Zonation at JB1 (Fig. 5), and the presence of a diffuse contact with the underlying gravels, suggests that these may reflect a continuation of sedimentation during MIS 7. No further robust Pleistocene ages were retrieved from JB2, however, an age of 135.8±23.9 ka was obtained from lacustrine material at JB1 (JB1-OSL8), which is taken to reflect an intensification of rainfall during MIS 5e. Zonation at JB1 suggests a marked change in deposition at 6.5

m (Unit 7), which we suggest reflects the onset of MIS 5e at ca. 130 ka. The basal marls of Zone II are finely laminated, loosely consolidated and friable, with some minor signs of haloturbation at lateral extensions of the unit, and with occasional gypsum lenses within Units 8 and 9, consistent with rapid drying phases. The upper section of Zone II is characterised by well-developed marls, which transition sharply into a well developed gypsum layer. This is overlain by Zone III, which is comprised of a thick diatomite layer featuring low $\delta^{18}O$ values, high silt and carbonate content with a band of humic silts at the lower contact. This likely represents the diatomaceous marls previously reported by Garrard et al. (1981) and dated by ^{14}C to 25,630±430 B.P. Diatoms assemblages within this unit reveal a diverse range of taxa with high relative abundances of benthic/epipelic taxon *Staurosirella pinnata var. pinnata, Staurosirella lapponica, Campylodiscus clypeus*. The occurrence of *Campylodiscus* and well-developed laminae throughout marl units are characteristic of fluctuating water levels at the site at this time. However, particularly high CA Axis 1 sample scores and the dominance of *Cyclotella distinguenda* and *Lindavia comensis* throughout this zone, also reveal a large shift in the planktonic: benthic ratio indicative of rising water levels and water body expansion.

A gradual shift towards more benthic and epipelic conditions at the top of Unit 10 at JB1 reflect a change from deep to shallow water conditions. Benthic and tychoplanktonic taxa within Unit 11 (e.g. *Nitzschia dissipata, Fragilaria famelica*) are typical of shallow, yet freshwater eutrophic lakes. Increased sand influx, higher $\delta^{18}O$ and $\delta^{13}C$ values (+6.08‰ and –4.9‰ respectively) as a result of evaporation (Leng and Marshall, 2004), decreased organic content and numerous well-developed gypsum lenses, also reflect a move to drier conditions and greater sensitivity to short-term P/E changes. At this point, lake water residence time was likely substantially reduced, with high evaporative losses and lower lake levels insufficient to dampen the effects of short-term climatic variations (e.g. Lamb et al., 2000; Leng and Marshall, 2004). It should be noted, however, that contributions from groundwater and/or infiltration from water bodies higher up the flow path make interpretation of the isotopic signal problematic, producing potentially unrepresentative values than would normally be produced from meteoric waters alone.

A feldspar age of 73.4±6.8 ka within Zone IV of JB1 (Unit 12) is consistent with increased regional rainfall during MIS 5a at ca. 80 ka, although it may be slightly older, as a subtraction method intended to circumvent environmental dose rate changes yields a low-precision estimate of 117.1 ± 51.2 ka. This phase of sedimentation comprises sandy marls characterised by generally high organic carbon content, numerous plant impressions and low $\delta^{18}O$ and $\delta^{13}C$ values. A successive peak in clay content corresponds to numerous calcretised plant remains, whilst a progressive enrichment of $\delta^{18}O$ (–5.5‰ to +2.8‰) and $\delta^{13}C$ (–11.1‰ to –4.3‰) values indicates a move towards shallower palustrine conditions. The presence of a dark, humic layer at 4.20 m supports the latter supposition and reflects the formation of black mats related to groundwater discharge, which generally form in wetland environments. The presence of *Rhopalodia constricta* indicates a shift to more brackish conditions, possibly reflecting a move to drier conditions at the end of MIS 5a. The occurrence of benthic species *Nitzschia dissipata, Rhopalodia constricta* and *Nitzschia angustata* also suggests shallower water depth. The unit is also characterised by high gypsum content; however, this is blocky, poorly developed and highly variable across profile, suggesting it may be diagenetic in origin, having formed at depth following the downward percolation of water during a subsequent wet phase. Other ages retrieved from Units 10-14 at JB1 seem to be significantly affected by uranium enrichment; therefore these are not considered reliable. Subtraction ages suggest that these units are likely to represent MIS 5 deposits, though it is possible that feldspar residuals have caused age overestimation and an MIS 3 age is certainly plausible (see Clark-Balzan et al., 2017).

A similar quartz age of 75.3±8.1 ka is reported from Zone III at JB3 (JB3-OSL4). A stratigraphically reversed age of 100.5±20.5 in Unit 7 (JB3-OSL3) was recorded at the interface between Zones III and IV at the site, and we suggest that both of these ages likely reflect an increase in rainfall during MIS 5a between ca. 85-75 ka. Given the higher elevation of JB3 (Fig. 2) and its distinctly basinal cross-sectional profile, it is likely that the sequence represents the formation of a smaller, isolated interdunal water body. This may have been contemporaneous with water body formation recorded at JB1; however, an absence of strict age controls inhibits this interpretation. At JB3, the three samples collected within carbonate-rich layers (JB3-OSL1—JB3-OSL3) yielded quartz D_e distributions with higher overdispersion values than expected based on results from nearby sites. We attribute the skewed distribution of JB3-OSL2 to partial bleaching and apply a minimum age model to calculate the D_e, and suggest that the symmetric but scattered distributions of samples JB3-OSL1 and JB3-OSL4 are more likely to relate to microdosimetric variation in the alpha and beta dose rates. The numerous shell fragments throughout the upper units may provide high and low dose rate regions (Kaufman et al., 1996); high dose rate minerals such as zircons are known to be present (Garzanti et al., 2013), and the unusually consolidated carbonates may have provided shielding to some grains (Nathan et al., 2003; 2008).

Unlike the other sequences within the Jubbah basin, JB3 indicates lake formation during global glacial conditions. Quartz ages from Zones IV and V of 66.3±8.0 and 56.2±8.3 respectively are consistent with lake formation during early MIS 3. Sedimentary characteristics and proxy values suggest a shift in lake water levels during this period, characterised by alternating gypsiferous marls, diatomite and well-developed gypsum layers. Numerous rhizoliths, dark humic bands and highly variable proxy values throughout the zone indicate fluctuating water levels at the site, followed by eventual lake desiccation. Conspicuous throughout Zone V are high concentrations of shells and shell fragments. These assemblages are predominantly composed of bivalves, notably *Cerastoderma* sp. and *Mytilopsis* sp, together with low concentrations of hydrobiid gastropods (*Hydrobia* cf. *lactea*) and occasional ostracods (*Cyprideis torosa*). The assemblage is typical of lagoons or estuaries, and is thus indicative of brackish conditions. The valves of *C. torosa* are smooth, indicating salinities higher than ~5 ‰. Both *Cerastoderma* and *Mytilopsis* are tolerant of a wide range of salinities, but are most often found in brackish waters. These bivalves can attain very high densities, in the case of *Cerastoderma* exceeding 13,000 individuals / m^2 (Legezynska and Wiktor, 1981), accounting for the richness of the samples recovered from the JB3 sequence.

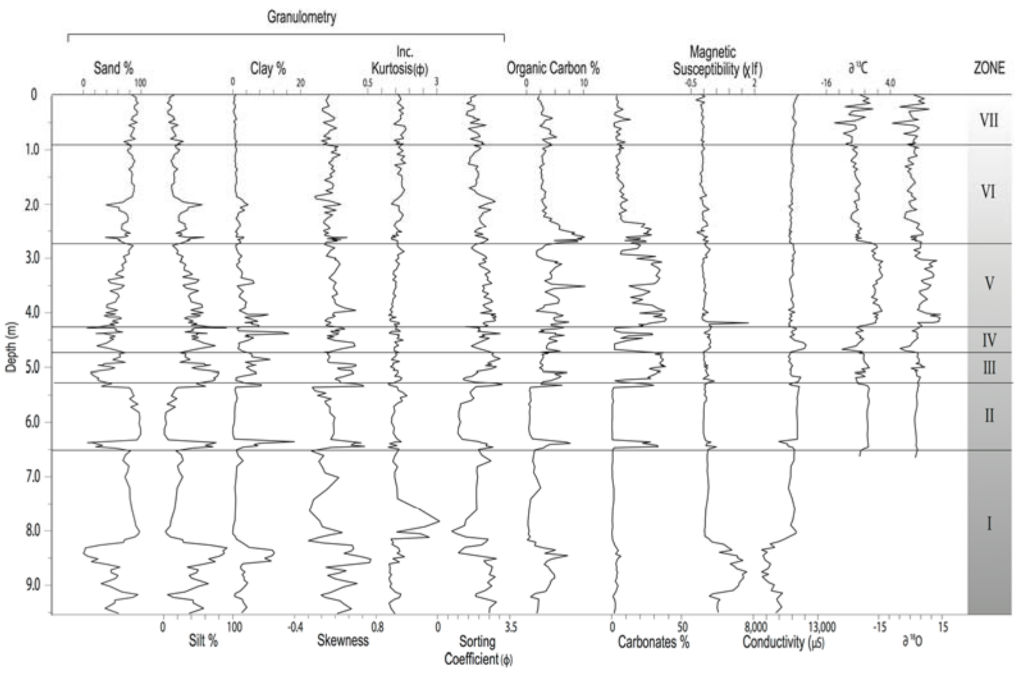

Figure 5: Multiproxy record from JB1.

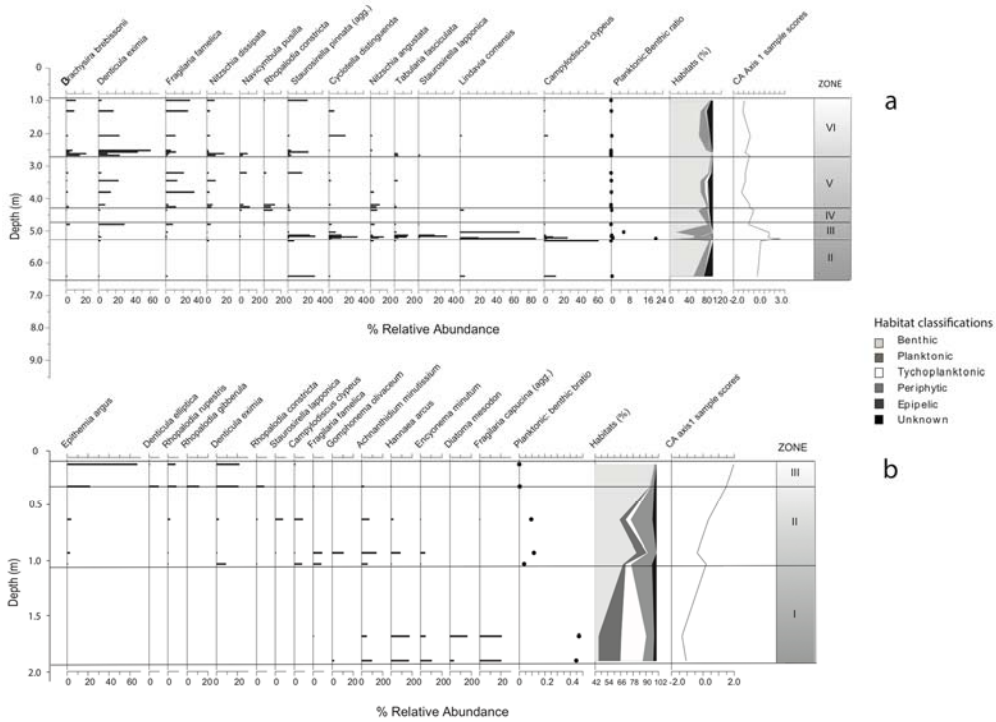

Figure 6: Diatom records from JB1 & ARY.

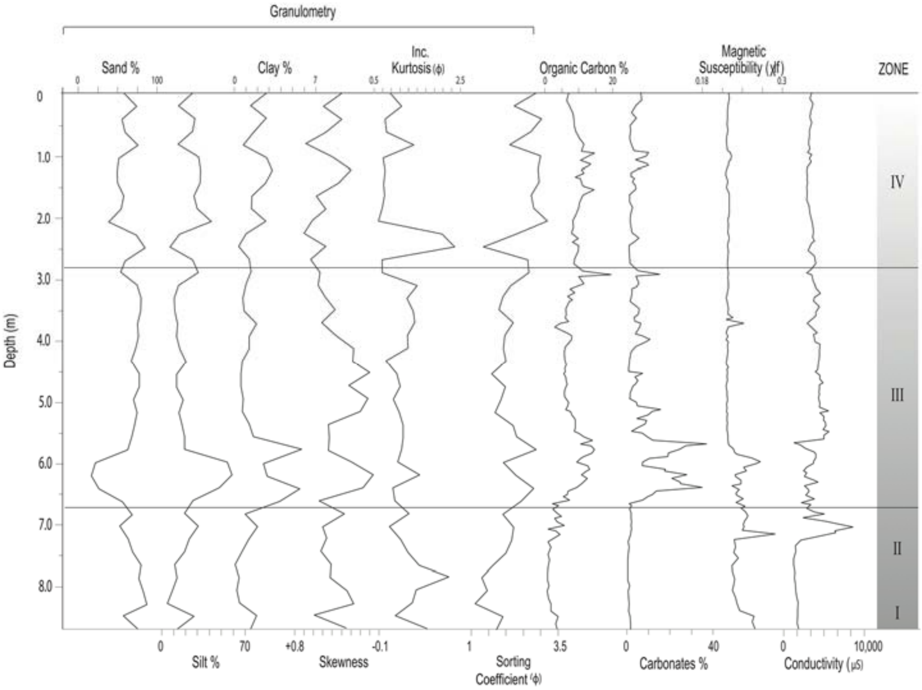

Figure 7: Multiproxy record from JB2.

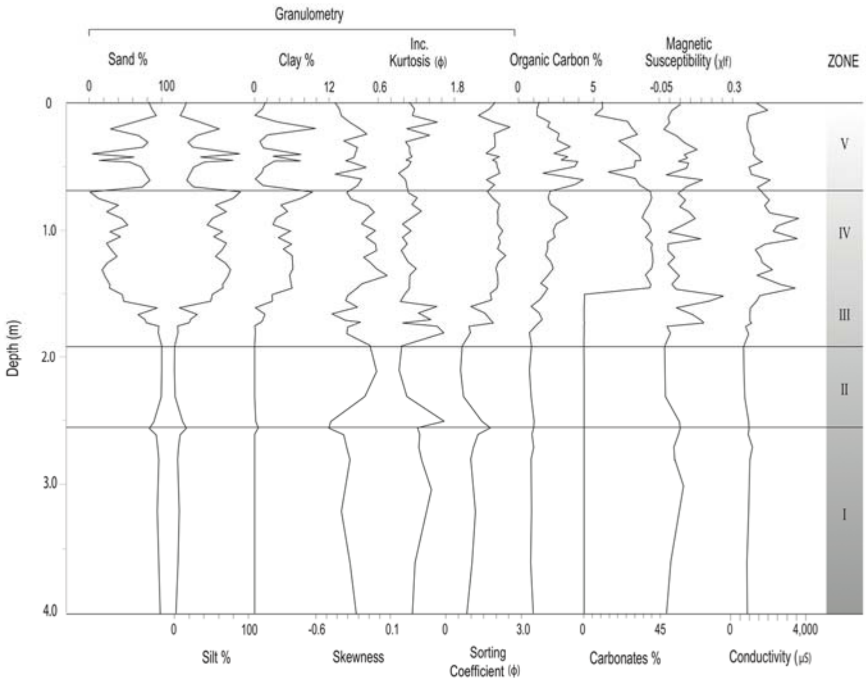

Figure 8: Multiproxy record from JB3.

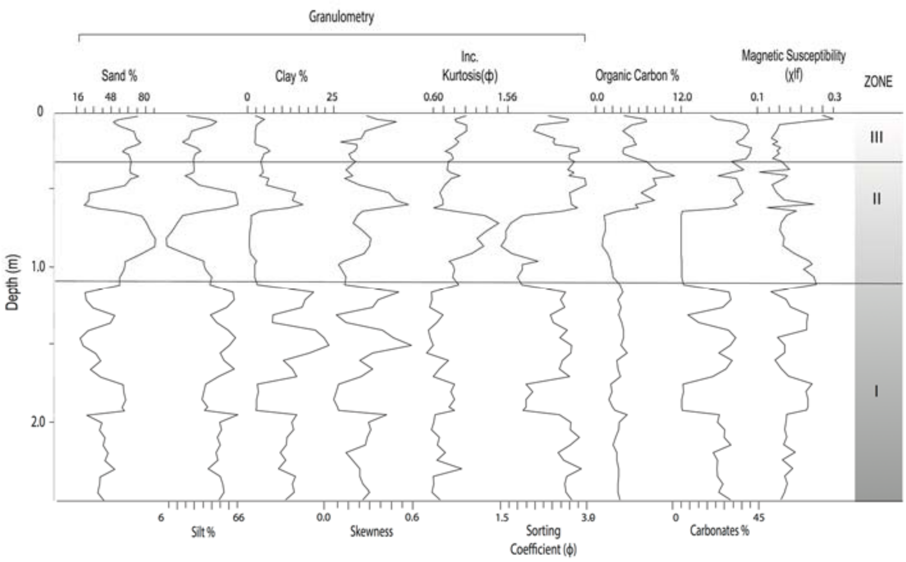

Figure 9: Multiproxy record from ARY.

4.2. Terminal Pleistocene and Holocene Proxy Records

Terminal Pleistocene-age deposits at Al Rabyah (ARY) comprise a series of low, inverted relief mesas capped by heavily indurated calcretes. The lowermost of these (Zone I) are composed of a thick sequence of marls featuring numerous root voids (Fig. 9), which transition sharply into moderately well sorted sands (Unit 3), suggesting a lowering of lake waters and an influx of aeolian material after 12.2±1.1 ka. This corresponds well with an age from the uppermost Zone IV at JB2 (Fig. 7), where a quartz age of 12.0±1.1 ka is derived from a well-developed gypsum layer overlying marls. Diatom assemblages bracketing Unit 3 at ARY reveal a dominance of *Hannaea arcus*, *Fragilaria capucina* and *Diatoma mesodon*, with a high ratio of planktonic taxa, and high abundances of tychoplanktonic species indicative of deeper, fresh waters immediately before and after ca. 12 ka, with low nutrient concentrations and little organic pollution (Fig. 6). Following a subsequent phase of expansion at ARY (Units 4-6), lake waters at the site appear to contract once again between around

11.4±0.8 ka to 6.6±0.7 ka, which is marked by increased sand influx and a decline in the planktonic: benthic ratio.

This is followed by a period of lake expansion from 6.5±05 ka, marked by the deposition of dark, humic silts. Diatom assemblages during this period are comprised of benthic taxa including *Denticula eximia*, *Fragilaria famelica, Rhopalodia, Epithemia argus* and *Achnanthidium minuitissium*, with a large decline in the planktonic: benthic ratio and a change in the CA Axis 1 sample scores. There is sparse ecological information on *Denticula eximia* although the genus *Denticula* occurs in diverse environments from those that are carbonate-rich with moderate conductivity to oligotrophic lakes. The presence of *Epithemia argus* and *Rhopalodia* within the upper units of ARY is indicative of nutrient-poor conditions, as these species may cohabit with nitrogen-fixing cyanobacteria enabling them to become abundant in low nitrogen conditions (Spaulding and Metzeltin, 2011; Meyers, 2014). Salinity levels also appear to have been relatively low during this period, since previous palaeoecological data from ARY confirm the predominance of freshwater conditions at the site during this time (Hilbert et al., 2014). Evidence from JB1 (Fig. 5 and 6) also indicates the presence of an early Holocene water body in the Jubbah basin. A radiocarbon age of 8980-8609 cal BP was retrieved from charred plant fragment material deposited within finely interdigitated marls and dark organic silts featuring numerous plant and root remains. This agrees well with quartz ages of 8.6±0.6 (JB2-OSL1) and 8.6±0.8 (JB2-OSL4) derived from gypsiferous marls at JB2 (Fig. 7), which is also coincident with the deposition of dark, humic silts. We propose that the upper ages from JB2 are reliable as they are indistinguishable at one sigma uncertainty. There is also a substantial hiatus in sedimentation between JB2-OSL4 (at ca. 4 m) and the underlying units when D_e values below and above this point are compared.

Proxy values during the early Holocene (Zone VI) at JB1 are somewhat invariant with respect to other zones, however, notable increases in silt, organic carbon and carbonates occur in Unit 17, corresponding with numerous root and plant impressions, indicative of fluctuating shallow water palustrine conditions in the basin during this time. $\delta^{18}O$ and $\delta^{13}C$ values display minor fluctuations throughout Zone VI, however, values are notably lower than Zone V, suggesting a phase of increasing groundwater discharge from ca. 9 ka. Diatoms assemblages indicate that the prevalent species during this period are benthic *Denticula exima, Brachysira brebissonii, Nitzschia dissipata* and *Fragilaria famelica,* which are reflected by the low planktonic: benthic ratio indicating shallower waters. *Denticula eximia*, *Nitzschia dissipata* and *Fragilaria famelica* occur in nutrient rich freshwater whereas *Brachysira brebissonii,* is common in moderately acidic (pH 4.7-5.8) to oligotrophic–mesotrophic lakes (i.e. 5.7-13.2 TP µg/L; Hamilton, 2010). However, high relative abundances of *Cyclotella distinguenda,* and the recurrence of *Lindavia comensis* suggest the return of some planktonic species. *Campylodiscus clypeus* also returns, highlighting increased alkalinity within the lake.

Gypsum development is conspicuous throughout the upper ~3 m at both JB1 and JB2; both of which feature long, needle-like prismatic crystals interdigitated with finely laminated sandy marls. Such growth typically occurs in a pure supersaturated, aqueous solution (i.e. water column), and although it is likely that some post-depositional crystal growth may also have occurred, laminations are generally well preserved, indicating that this is minimal. The presence of interdigitated wavy laminations of marls and gypsum throughout the upper ca. 2 m of JB1 may be indicative of seasonal lake level changes or subaerial aeolian scour. The prevalence of shallow, seasonally astatic water levels featuring regular evaporitic phases is also supported by large shifts in $\delta^{18}O$ and $\delta^{13}C$ values throughout the upper ~1 m at JB1 (–9.3‰ to +8.2‰ and –13.5‰ to –1.4‰ respectively).

5. Discussion

5.1. Controls on Lake Formation and Wetland Development in the Jubbah Basin

The Jubbah basin records exhibit exceptional sedimentary depths in comparison to other lake records from Arabia, and are currently unique in recording water body formation within the same basin during both glacial and interglacial periods. We suggest that this is the result of specific geomorphological controls, which have facilitated the repeated formation of a water body in an oasis setting over the past ca. 360 kyr. The presence of sandstone outcrops has sheltered the basin from dune encroachment, providing the necessary accommodation space for water body formation. Lake and wetland development would have also been driven by groundwater recharge from the Saq aquifer through focussed recharge from springs, such as those identified near the base of Jebel Qatar (i.e. JQ-101 (Crassard et al., 2013)). As such, rainfall changes in the Saq sandstone recharge area to the west of the region may at times have played a more important role in the formation of water bodies within the basin than local precipitation. Given the moderately long (100-300 km) flow paths to the recharge area, however, it should be expected that there might have been a considerable lag between any climatic variation recorded at Jubbah, and spring discharge response. Unfortunately, while the ages reported here for increased rainfall occur in line with other records from the region, the associated errors prohibit further comment on this potential lag. It is likely that such recharge events were episodic, however, and that groundwater recharge may have extended the period through which water entered the basin beyond wet periods.

In addition, infiltration of precipitation through the surrounding dunes, including water contained within perched water bodies, will have also played an important role in lake water recharge. The surrounding deep (up to 60 m thick) dunes absorb and retain even minor levels of precipitation below the evaporation zone, with approximately 25% of rainfall effectively infiltrating into depressions down through the sand (e.g. Dincer et al., 1974). It should be noted that the underlying bedrock depression might in fact continue beneath the surrounding dunes for an unknown distance, hence accumulating infiltration from a large area of the dune field and supporting the presence of a local perched aquifer system at Jubbah, however, the extent of the underlying depression remains uncertain. While the density of vegetation within the surrounding dune field would have been greater during wetter periods, moisture losses due to transpiration by plants may have only played a minor role in the overall water balance of the dunes. As such, it is likely that the areal extent of water bodies within the Jubbah basin was determined by the balance between spring discharge, evaporative losses, and marginal seepage into the dry (unsaturated) dune sand sediments.

It is important to note that there is considerable contention surrounding the usage of the term 'lake', and a strict definition with respect to arid regions such as Arabia, is lacking. The criteria set out by Enzel et al. (2012; 2015), namely that wetlands comprise 'marshy or shallow water environments' and lakes 'open water bodies' is based upon typical geomorphic environments, depositional and erosional shoreline features, basin sediments and biological remains of both types in arid regions (Engel et al., 2017). However, these criteria apply predominantly to arid landscapes dominated by structural forms, as opposed to interdunal water bodies in soft sand seas. A lack of features such as shorelines is problematic in soft sediment areas, particularly when factors such as human development and dune reactivation along the fringes of interdunal basins are considered (e.g. Engel et al., 2017). Unfortunately, there is little clarification as to the hydrological and hydrographic criteria such as water depth, spatial extent, trophic ecology, or seasonal/interannual response that would otherwise distinguish one type of water body from another. Indeed, the lower limit size of standing (lentic) water bodies, which qualify as 'lakes', may be as low as 0.01-0.1 km^2 (Engel et al., 2017). When considering the residence time of such water bodies, a distinction is made between lakes as being permanent (year round, persisting for years to centuries), and wetlands as being ephemeral (i.e. seasonal). In this respect, previous findings from Al Rabyah (ARY) at Jubbah (Hilbert et al., 2015) and Tayma (Engel et al., 2012; Ginau et al., 2012), support the notion of permanent water bodies in the region during the early Holocene, while faunal remains such as fish and tortoise from Ti's al Ghadah in the western Nefud (Thomas et al., 1998; Rosenberg et al., 2013) point towards similar permanency during Pleistocene pluvial periods. As such, while some contention continues to surround this issue, we believe that the apparent perennial nature of these water bodies is nonetheless indicative of a markedly increased precipitation regime (albeit greatly facilitated by groundwater discharge), which was sufficient to overcome evaporative losses and allow lake formation.

5.2. Phases of Lake Formation and Wetland Development

Increased precipitation occurred in line with interglacials MIS 11 or 9, 7, 5 and 1, with further lake development occurring during early MIS 3. At 359.4±84.3 ka, sedimentation within the basin was characterised by a thick sequence of green clayey silt/sands, formed by the weathering of silicate material from the Saq sandstone and long-term accumulation under still water conditions. In addition, seasonal infiltration and groundwater recharge would have led to sub-surface weathering, in particular oxidation and carbonate dissolution, leading to the accumulation of insoluble clays in the lowest areas of the basin (e.g. Wood and Osterkamp, 1987). The homogeneity, thickness and distribution of these facies across the basin at both JB1 and JB2 suggest that a large lentic water body occupied the basin during this time. While this broadly concurs with other studies from the region for both MIS 11 and MIS 9 (e.g. Rosenberg et al., 2013), it is unclear, given the potential age range, as to which period is represented at this point within the Jubbah basin. Elsewhere within the Nefud, ages of ca. 366 and 325 ka from beneath extensive diatomite deposits (Rosenberg et al., 2013) are taken to indicate lake formation during MIS 9, which was characterised by undisturbed freshwater depositional conditions several metres deep. Given that the thick sequence of clays dated to ca. 360 ka at Jubbah are potentially overlain by deposits dated to MIS 7 (based on stratigraphic conformity at JB1 and JB2), and that any interpretation of the sediments being of MIS 11 age necessitates an explanation as to the conspicuous absence of MIS 9 within the Jubbah record, it is likely that formation during the latter period is more plausible. During MIS 7, sedimentation within the Jubbah basin was characterised by the erosion and mobilisation of slope material from the adjacent sandstone outcrops. At this point the basin would have exhibited a deeper profile with greater slope gradient and increased runoff potential. Evidence for wetter conditions in the basin during MIS 7 is also reported by Petraglia et al. (2012) (Fig. 2), and to the west of Jubbah by Rosenberg et al. (2013).

The onset of MIS 5e is marked by the existence of a large freshwater water body in the basin, which likely fluctuated as a result of seasonal rainfall changes and/or variations in spring discharge. The MIS 5e lake phase at Jubbah terminates with a shift to shallower benthic conditions driven by reduced lake water residence times, greater sensitivity to short-term P/E changes and higher evaporative losses. OSL ages do not support previous estimates by Garrard et al. (1981), which suggest that lake formation occurred at ca. 25 ka. It is likely that this underestimation is the result of contamination by younger ^{14}C from meteoric waters (Rosenberg et al., 2013). Hydroclimatic conditions during MIS 5a indicate an initial expansion of lake waters within the Jubbah basin, followed by a lowering of lake levels. Palaeoecological data indicate that the wider basin likely comprised a predominantly wetland environment at this time, characterised by increasingly saline, brackish conditions and chemically concentrated and anoxic bottom waters (e.g. Morellón et al., 2008). The record from JB3 also indicates the formation of a smaller, less evaporitic, perched interdunal water body during MIS 5a, which was disconnected from the main basin. An early MIS 3 pluvial phase from ca. 60 ka is also recorded within the Jubbah basin, and is characterised by palustrine/wetland conditions with fluctuating water levels, which concurs with recent finding from the Al Marrat basin ~50 km southwest of Jubbah (Fig. 1) (Jennings et al., 2016). We suggest that in a similar situation to that of Al Marrat, water body formation at this time was likely facilitated by recharge from the Saq aquifer, during what may have been a relatively brief and weaker wet phase, in comparison to those occurring during interglacials.

Palaeoecological evidence indicates the presence of a freshwater lake at the western end of the basin around the Terminal Pleistocene/Holocene transition at ca. 12 ka, with a high ratio of planktonic taxa, and high abundances of tychoplanktonic species indicative of deeper, fresh waters. Water levels within the wider basin during the Early Holocene between ca. 12 and 9 ka were astatic and evaporitic, featuring predominantly eutrophic diatom species indicative of a more saline and shallow wetland environment. Shallow but freshwater conditions appear to have persisted across the wider basin from ca. 9 ka, with fluctuating lake levels and a predominance of benthic taxa. However, the presence of freshwater mollusc species *Gyraulus convexiusculus* at ARY, along with well-developed non-gypsiferous marls both there and at JQ101 (Crassard et al., 2013), confirm the persistence of freshwater bodies in the basin until ca. 6.5 ka.

Given the longevity and apparent sensitivity of the Jubbah records it is reasonable to consider the potential continuity of water body formation in the basin between pluvial periods. Jubbah's history as an oasis town, and the presence of groundwater near the modern surface until recent historic times, suggests that only minor rainfall increases were necessary to produce standing water within the basin. Indeed, palaeohydrological modelling at the Tayma oasis suggests that just 150 ±25 mm was required to initiate lake formation during the early Holocene (Engel et al., 2011). This figure is similar to the current peninsula-wide average of ~140 mm (Almazroui et al., 2013), with Jubbah itself located within 100-200 mm annual rainfall range. Furthermore, in climate model simulations for 21 ka (LGM), Jubbah remains within this rainfall range (Jennings et al., 2015), possibly as a result of winter storms related to Mediterranean depressions and cyclogenesis west of the Zagros Mountains (Barth & Steinkohl, 2004). In the absence of historic and recent intensive irrigation practices, therefore, it is possible that the unique geomorphological properties of the Jubbah basin would allow shallow water conditions to persist with only minimal amounts of rainfall. Nonetheless, while the record from Jubbah is deep with respect to other records from Arabia, sedimentation within the basin would not have been continuous over the past ca. 360 ka. The Jubbah depression would have been susceptible to substantial deflation during intervening arid phases, leading to hiatuses in deposition between wetter periods. It is also likely that only sediments that have undergone extensive diagenetic alteration and induration have been preserved, leading to the preferential preservation of younger sediments, and large discontinuities present in older material. As such, there is the potential for gaps to occur within those parts of the sequences that represent phases of pre-Holocene rainfall increases, since much of the material recording these periods may have been lost. Despite this, the correspondence of water body formation within the Jubbah basin with the wider palaeoclimatic record of Arabia provides an important means through which to assess regional climatic changes during the Mid-Late Pleistocene and Holocene periods.

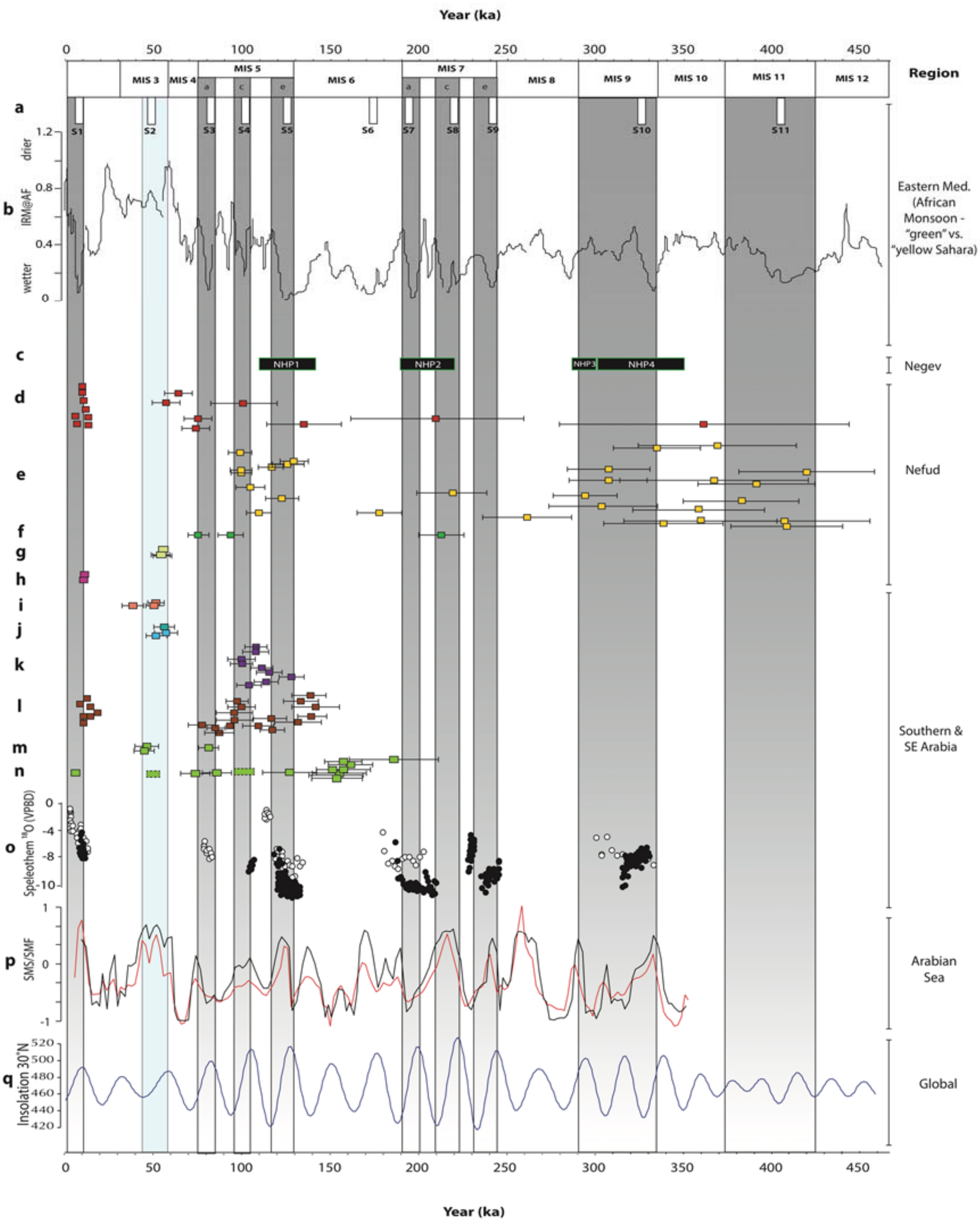

Figure 10: Summary and comparison of key palaeoclimate records from in and around the Arabian Peninsula. (a) Eastern Mediterranean sapropels (Zhao et al., 2011); (b) dust flux related to wet-arid ("green" vs. "yellow" Sahara) monsoon-driven cycles (Larrasoaña et al., 2003); (c) Negev Humid Periods derived from speleothem records (Vaks et al., 2010); (d) Lake/wetland ages from Jubbah (this study); (e) Nefud palaeolake ages (Rosenberg et al., 2013); (f) inferred lake age formation at archaeological site JQ1 at Jubbah (Petraglia et al., 2012); (g) wetland ages reported from the Nefud (Jennings et al., 2016); (h) ages of oasis development at Tayma (Engel et al., 2011); (i) ages of fluvial channel activation from central Saudi Arabia (McLaren et al., 2008); (j) ages from fluvio-lacustrine sequence in eastern UAE (Parton et al., 2013); (k) ages of lake formation from Saiwan, Oman (Rosenberg et al., 2012); (l) reported lake ages from Mundafan and Khujaymah, southern Rub al Khali (Rosenberg et al., 2011); (m & n) ages for the activation of the Al Ain alluvial fan system, eastern UAE, at Remah (m) (Farrant et al., 2012) and Al Sibetah (n) (Parton et al., 2015a); (o) Speleothem $\delta^{18}O$ records from Mukalla and Hoti Cave (summarized in Fleitmann et al., 2011); (p) summer monsoon stack (SMS) and summer monsoon factor (SMF) of monsoon intensity proxies from the Arabian Sea (Clemens and Prell, 2003); (q) June insolation at 30°N (Berger and Loutre, 1991).

5.3. Jubbah and the wider Arabian Palaeoclimate Record

Interglacial-age lake formation at Jubbah corresponds well with numerous palaeoclimatic and palaeoenvironmental studies, while glacial age lake development during MIS 3 supports a growing number of records attesting to a weaker wet period during early MIS 3. Widespread lake/wetland development is reported from elsewhere in the western Nefud during peak interglacials (e.g. Rosenberg et al., 2013; Stimpson et al., 2016), in particular MIS 11, 9, 7 and 5, however, MIS 1 lake formation appears to have been restricted to oases settings such as those at Jubbah (Crassard et al., 2013; Hilbert et al., 2014) and Tayma (Engel et al., 2011; Ginau et al., 2012). Broadly this concurs with the wider Arabian palaeoclimatic record (Fig. 10), which reveals an activation of hydrological systems across the peninsula during eccentricity-paced interglacial maxima. In southern and southeastern regions speleothem and lake records reveal an intensification and northward displacement of the summer ITCZ and associated monsoon rainfall (e.g. Burns et al., 2001; Fleitmann et al., 2003; 2011; Fleitmann and Matter, 2009; Matter et al., 2015; Parker et al., 2004; 2006; 2016; Preston et al., 2015; Rosenberg et al., 2011; 2012;), along with the widespread activation of extensive alluvial fans and drainage processes (Blechschmidt et al., 2009; Parton et al., 2015a; Matter et al., 2016). The phasing of terrestrial rainfall increases corresponds well with marine records of summer monsoon proxies from the Arabian Sea (e.g. Clemens and Prell, 2003; Des Combes et al., 2005; Clemens et al., 2010), which show an abrupt decrease in dust influx, and increased nutrient supply and upwelling. In the Red Sea region, an intensified EASM led to freshwater influxes and lowered surface salinities (e.g. Badawi, 2014) with a substantially altered wind regime across the region (Trommer et al., 2011) and high summer-winter temperature ranges (e.g. Felis et al., 2004). Similarly, speleothem records from the Negev reflect the strengthening of eastern Mediterranean cyclones during interglacials, producing annual precipitation in excess of 300 mm (e.g. Bar-Matthews et al., 2003; Vaks et al., 2010). The palaeoclimatic picture of Arabia during interglacials, therefore, is one of widespread hydrological amplification featuring freshwater lakes, spatially extensive perennially flowing rivers (e.g. Parton et al., 2015a; Matter et al., 2016) and vegetation development.

While substantial northward displacements of the ITCZ and Indian Ocean Summer Monsoon (IOSM) were the likely source of rainfall in southern and eastern regions of

Arabia, it is unlikely that the IOSM rainfall belt reached ~27° N (e.g. Rosenberg et al., 2013; Enzel et al., 2015). While a potential contribution of rainfall from synoptic conditions associated with Red Sea troughs cannot be discounted (e.g. Waldmann et al., 2010), we concur with other studies (e.g. Herold and Lohmann, 2009; Jennings et al., 2015; Parton et al., 2015b), which suggest that eastward zonal moisture transport from an intensified East African Summer Monsoon (EASM) was likely the key source of rainfall across the Nefud. Precipitation estimates of MIS 5e interglacial rainfall derived from an ensemble of climate model simulations suggest that annual rainfall in the region may have been up to 400 mm, with contributions from both African monsoon and Westerly sources (Jennings et al., 2015). For the current interglacial, numerous palaeoenvironmental archives support widespread climatic amelioration. Recent COSMOS and HOL6 climate models (Guagnin et al., 2016) indicate a substantial increase in rainfall at 8 ka BP, and in a similar scenario to MIS 5e, a northward extension of the EASM was the most likely source of rainfall. Climate simulations suggest that annual precipitation during this time was highly variable, ranging from lows of 20 mm to highs of 420 mm (Guagnin et al., 2016).

The environmental picture during glacials, however, is less clear. For early MIS 3, a HadCM3 palaeoprecipitation model suggests that glacial-age rainfall in the region may have been less than 100 mm, although the extension of the East African Summer Monsoon is likely underestimated (Jennings et al., 2016). Previously it was assumed that climatic conditions in Arabia during global glacial periods were too arid to sustain lake development (e.g. Fleitmann et al., 2011; Rosenberg et al., 2011). While marine evidence from the Arabian Sea (e.g. Clemens and Prell, 2003; Des Combes et al., 2005; Caley et al., 2011a) suggests that IOSM maxima are in phase with precessionally regulated summer insolation, the limited terrestrial expression of this linkage has been used to suggest that precipitation and wind strength may be decoupled during glacials (Fleitmann et al., 2011). A growing corpus of evidence from southern and southeastern Arabia, however, now indicates that pluvial periods occurred during glacials MIS 6 at ca. 160-150 ka (e.g. Wood et al., 2003; Preusser et al., 2002; Parton et al., 2015) and early MIS 3 at ca. 55 ka (e.g. Krbetschek, 2008; Blechschmidt et al., 2009; Farrant et al., 2012; Parton et al., 2013; 2015a; Hoffmann et al., 2015). While all of these records reflect a strengthening of the glacial-age IOSM, resolving the source of rainfall during MIS 3 within northwestern Arabia remains problematic. African monsoon records appear to reflect increased monsoon intensity during early MIS 3 (e.g. Trauth et al., 2003; Revel et al., 2010; Rohling et al., 2013), synchronous with increased Nile discharge and the deposition of sapropel unit S2 (Williams et al., 2015). However, the presence of this 'debated' sapropel within the Eastern Mediterranean at ca. 55 ka may also be attributable to increased stratification in the Mediterranean, as opposed to increased monsoon-fed Nile discharge (see Rohling et al., 2015 for comprehensive review). In addition, evidence for a wet phase at ca. 60 ka from speleothem records in Libya (Hoffmann et al., 2016), suggest that the correspondence between a precessionally controlled monsoon and enhanced convergence at 25-40°N as a consequence of Hadley Cell contraction, may account for increased regional rainfall at this time.

As such, it remains unclear as to whether the records presented here support other findings from the Nefud (Jennings et al., 2016), which suggest an intensification of the EASM between ca. 55-60 ka. Further, the occurrence a precessional minimum at ca. 60 ka, and an obliquity maximum at ca. 50 ka also problematize the assignment of a predominant moisture source for the region during early MIS 3. Caley et al. (2011b) highlight regional differences in the timing of the Indian and East African monsoons, suggesting that while IOSM records contain a stronger obliquity signal, the EASM responds more closely to precessional forcing. Nonetheless, while the moisture source/s may remain uncertain for this period, it is likely that a strong contribution of groundwater recharge, alongside small increases in precipitation, and reduced evaporation, contributed to wetland development within the Nefud during early MIS 3.

6. Conclusions

The hydroclimatic records in the Jubbah basin comprise a unique sequence of deposits that demonstrate lake/wetland formation over multiple interglacials and during MIS 3. The longevity of the record at Jubbah, and the apparent sensitivity to regional rainfall increases is likely a result of the basin's unique geomorphological setting. Protected from the eastward transport of aeolian material, the depression has not been susceptible to substantial infilling by the surrounding dunes. In addition, diffuse and focussed groundwater recharge, have contributed to lake/wetland formation during wet phases, with a potentially stronger groundwater influence during MIS 3.

Our findings have numerous implications for understanding human demographic and behavioural change. The identification of Middle Pleistocene wet periods at Jubbah demonstrates windows of opportunity for hominins using Acheulian technology, and by MIS 7, Middle Palaeolithic technology. The wet phases of MIS 5e, 5a and early MIS 3 are associated with repeated hominin occupations of Jubbah and the surrounding area (e.g. Petraglia et al., 2012; Groucutt et al., 2017; Jennings et al., 2016). The significant technological differences between these assemblages are consistent with their production by different populations, and probably species, of hominins. The demonstration of pluvial conditions in northern Arabia in early MIS 3, for instance, highlights the possibility that this area may have witnessed admixture between *Homo sapiens* and Neanderthals, which is widely argued to have occurred somewhere in southwest Asia ~60-50 ka (e.g. Green et al., 2010). Moving into the Holocene, evidence from Jubbah demonstrates periodic lake formation between ca. 12 and 6 kyr BP, which thus far has not been identified in smaller depressions in the dunefield (Rosenberg et al., 2013), and is likely tied to oasis development. This is in keeping with growing evidence for a 'weak connection' between Arabia and the Levant at this time, where there was some cultural diffusion from the north but perhaps relatively minor population dispersal into Arabia. These findings indicate that across the various wet phases of the Pleistocene and Holocene there was not a single kind of human response to climate change. Rather, responses depended on the nature of the environmental change and the kinds of adaptations employed by humans. Never the less, the climatic shifts identified in the Jubbah basin provide significant context to changes in human demography. Just as seeking to understand environmental conditions between peak wet periods remains a key area of research (i.e. how much water was available in places such as Jubbah between interglacials), so understanding human-environment connections in these time periods offers a key area to research. Did human populations become regionally extinct during dry phases? To what extent did oases such as Jubbah buffer populations through these phases? With increasing data available on the peak-wet phases of Arabia, such questions must animate future research in the area and allow the story of long-term interaction between humans and the environment to be told. In addition, the continually expanding palaeoclimatic picture from Arabia is one of increasing spatio-temporal heterogeneity heavily influenced by regional topographic and climatic controls, and not confined to a simplistic wet-dry dichotomy.

Acknowledgements

Over the last few decades the field of palaeolimnology has been significantly enhanced by the use of stable isotopes. Neil Roberts and Henry Lamb (for whom the collection of papers in this volume is dedicated) were at the forefront of this advancement amongst UK researchers, applying relatively new techniques to lakes in Africa and the Mediterranean. This study is no small way benefits from their trail blazing research. We also thank His Royal Highness Prince Sultan bin Salman, President of the Saudi Commission for Tourism and National Heritage (SCTH), and Prof. Ali Ghabban, Vice President for Antiquities and Museums, for permission to carry out this research. We thank our Saudi colleagues from the SCTH, especially Jamal Omar, Sultan Al-Fagir, and Abdulaziz al-Omari for their support and assistance with the field investigations, and two anonymous reviewers for their insightful and constructive assessments of an earlier version of the manuscript. Financial support for the fieldwork and project was provided by the European Research Council (ERC) (grant number 295719, to MDP) and the SCTH. HSG thanks the British Academy for funding.

References

Al-Salamah, Ibrahim, S., Ghazaw, Y.M. and Ghumman, A.R., 2011. Groundwater modeling of Saq Aquifer Buraydah Al Qassim for better water management strategies. Environmental monitoring and assessment, 173(1), 851-860.

Almazroui, M., Abid, M. A., & Athar, H., 2013. Interannual variability of rainfall over the Arabian Peninsula using the IPCC AR4 Global Climate Models - Almazroui - 2012 - International Journal of Climatology - Wiley Online Library. International Journal of Climatology 33, 2328-2340.

Alsharhan, A.S., Rizk, Z.A., Nairn, A.E.M., Bakhit, D.W. and Alhajari, S.A. eds., 2001. Hydrogeology of an arid region: the Arabian Gulf and adjoining areas. Elsevier.

Auclair, M., Lamohe, M., Huot, S., 2003. Measurement of anomalous fading for feldspar IRSL using SAR. Radiat. Meas. 37, 487–492. doi:10.1016/S1350-4487(03)00018-0

Badawi, A., 2014. Late quaternary glacial/interglacial cyclicity models of the Red Sea. Environmental Earth Sciences. ISSN: 1866-6280 1-17. doi.org/ 10.1007/s12665-014-3446-8.

Bar-Matthews, M., Ayalon, A., Gilmour, M., Matthews, A., Hawkesworth, C.J., 2003. Sea- land oxygen isotope relationships from planktonic foraminifera and spe-leothems in the eastern Mediterranean region and their implication for pale- orainfall during interglacial intervals. Geochimica et Cosmochimica Acta 67, 3181-3199.

Barth, H.J., Steinkohl, F., 2004. Origin of winter precipitation in the central coastal lowland of Saudi Arabia. Journal of Arid Environments 5, 101-115.

Barthélemy, Y., Béon, O., le Nindre, Y.M., Munaf, S., Poitrinal, D., Gutierrez, A., Vandenbeusch, M., Al Shoaibi, A. and Wijnen, M., 2007. Modelling of the Saq aquifer system (Saudi Arabia). Aquifer Systems Management: Darcy’s Legacy in a World of Impending Water Shortage. Taylor & Francis, London, pp.175-190.

Battarbee, R., 2000. Palaeolimnological approaches to climate change, with special regard to the biological record. Quaternary Science Reviews, 19(1-5), 107–124.

Battarbee, R. W., Jones, V. J., Flower, R. J., Cameron, N. G., Bennion, H., Carvalho, L. and Juggins, S., 2001. Diatoms. In: J. P. Smol, Birks, H. J. B. and Last, W. M. (eds) Tracking Environmental Change Using Lake Sediments, Volume 3: Terrestrial, Algal and Siliceous Indicators. Dordrecht, The Netherlands, Kluwer Academic Publishers. 155-202.

Bennett, K.D. (1996) Determination of the Number of Zones in a Biostratigraphical Sequence. New Phytologist, 132(1), 155-170.

Berger, A., Loutre, M.F., 1991. Insolation values for the climate of the last 10 million years. Quaternary Science Reviews 10 (4), 297-317.

Blechschmidt, I., Matter, A., Preusser, F., Rieke-Zapp, D., 2009. Monsoon triggered formation of Quaternary alluvial megafans in the interior of Oman. Geomorphology 110, 128-139.

Blunt, L.A., 1881. A Pilgrimage to Nejd: The Cradle of the Arab Race (Vol. 1). J. Murray.

Bramkamp, R.A., Brown, G.F., Holm, D.A. and Layne Jr, N.M., 1963. Geologic map of the Wadi as Sirhan quadrangle, Kingdom of Saudi Arabia (No. 200-A). US Geological Survey.

Breeze, P., N. A. Drake, R. G. Jennings, A. Parton, H. S. Groucutt, L. Clark-Balzan, C. Shipton, T. White, M. D. Petraglia, and A. Alsharekh. 2015. Remote Sensing and GIS Techniques for Reconstructing Arabian Paleohydrology and Identifying Archaeological Sites. Quaternary International 382, 98–119.

Bronk Ramsey, C., Higham, T.F.G., Owen, D.C., Pike, A.W.G., Hedges, R.E.M., 2002. Radiocarbon dates from the Oxford AMS system: Archaeometry Datelist 31. Archaeometry 44, 1–149.

Bronk Ramsey, C., Higham, T., Leach, P., 2004. Towards high-precision AMS: Progress and limitations. Radiocarbon 46, 17–24.

Bronk Ramsey, C., 2009. Bayesian analysis of radiocarbon dates. Radiocarbon 51, 337–360.

Burns, S.J., Fleitmann, D., Matter, A., Neff, U., Mangini, A., 2001. Speleothem evidence from Oman for continental pluvial events during interglacial periods. Geology 29 (7), 623–626.

Caley, T., Malaize, B., Zaragossi, S., Rossignol, L., Bourget, J., Eynaud, F., Martinez, P., Giraudeau, J., Charlier, K., Ellouz-Zimmermann, N., 2011a. New Arabian Sea records help decipher orbital timing of Indo-Asian monsoon. Earth and Plan- etary Science Letters 308 (3e4), 433-444.

Caley, T., Malaize, B., Revel, M., Ducassou, E., Wainer, K., Ibrahim, M., Shoeaib, D., Mi- geon, M., Marieu, V., 2011b. Orbital timing of the Indian, East Asian and African boreal monsoons and the concept of a “global monsoon”. Quaternary Science Reviews 30, 3705-3715.

Clark-Balzan, L., 2016. Source and characteristics of blue , infrared (IR), and post-IR IR stimulated signals from gypsum-rich samples. Anc. TL 34, 6–13.

Clark-Balzan, L., Parton, A., Breeze, P.S., Groucutt, H.S. and Petraglia, M.D., 2017. Resolving problematic luminescence chronologies for carbonate-and evaporite-rich sediments spanning multiple humid periods in the Jubbah basin, Saudi Arabia. Quaternary Geochronology, *in press,* doi: 10.1016/j.quageo.2017.06.002.

Clemens, S., Prell, W.L., 2003. A 350,000 year summer-monsoon multi-proxy stack from the Owen Ridge, Northern Arabian Sea. Marine Geology 201, 35-51.

Clemens, S.C., Prell, W.L., Sun, Y., 2010. Orbital-scale timing and mechanisms driving Late Pleistocene Indo-Asian summer monsoons: reinterpreting cave speleothem d18O. Paleoceanography 25, PA4207. doi.org/10.1029/2010PA001926.

Crassard, R., Petraglia, M.D., Parker, A.G., Parton, A., Roberts, R.G., Jacobs, Z., Alsharekh, A., Al-Omari, A., Breeze, P., Drake, N.A., Groucutt, H.S., Jennings, R., Régagnon, E., Shipton, C., 2013. Beyond the Levant: first evidence of a pre-pottery Neolithic incursion into the Nefud Desert, Saudi Arabia. PLoS ONE 8 (7), e68061.

Dean Jr, W.E., 1974. Determination of carbonate and organic matter in calcareous sediments and sedimentary rocks by loss on ignition: comparison with other methods. Journal of Sedimentary Research, 44(1).

Dearing, J., 1999. Magnetic susceptibility. Environmental magnetism: A practical guide, 6, pp.35-62.

Des Combes, H.J., Caulet, J.P., Tribovillard, N., 2005. Monitoring the variations of the Socotra upwelling system during the last 250 kyr: a biogenic and geochemical approach. Palaeogeography, Palaeoclimatology, Palaeoecology 223, 243-259.

Dill, H.G., 2011. A comparative study of uranium – thorium accumulation at the western edge of the Arabian Peninsula and mineral deposits worldwide. Arab. J. Geosci. 4, 123–146. doi:10.1007/s12517-009-0107-4

Dincer, T., Al-Mugrin, A., & Zimmermann, U., 1974. Study of the infiltration and recharge through the sand dunes in arid zones with special reference to the stable isotopes and thermonuclear tritium. Journal of Hydrology, 23, 79-109.

Duller, G.A.T., 2003. Distinguishing quartz and feldspar in single grain luminescence measurements. Radiat. Meas. 37, 161–165. doi:10.1016/S1350-4487(02)00170-1

Durcan, J.A., King, G.E., Duller, G.A. T., 2015. DRAC: Dose Rate and Age Calculator for trapped charge dating. Quat. Geochronol. 28, 54–61. doi:10.1016/j.quageo.2015.03.012

Engel, M., Brückner, H., Pint, A., Wellbrock, K., Ginau, A., Voss, P., Grottker, M., Klasen, N., Frenzel, P., 2011. The early Holocene humid period in NW Saudi Arabia – Sediments, microfossils and palaeo-hydrological modelling. Quaternary International. doi.org/10.1016/j.quaint.2011.04.028

Farrant, A.R., Ellison, R.A., Thomas, R.J., Pharaoh, T.C., Newell, A.J., Goodenough, K.M., Lee, J.R., Knox, R.O., 2012. The geology and geophysics of the United Arab

Emirates. In: Geology of the Western and Central United Arab Emirates. British Geological Survey, vol. 6. Keyworth, Nottingham, p. 371.

Faure, G., 1986. Principles of Isotope Geology (2nd ed.). John Wiley & Sons, New York.

Felis, T., Lohmann, G., Kuhnert, H., Lorenz, S.J., Scholz, D., Patzold, J., Al-Rousan, S.A., Al-Moghrabi, S.M., 2004. Increased seasonality in Middle East temperatures during the Last Interglacial period. Nature 429, 164-168.

Fisk, E.P. and Pim, R.H., 1985.Hydrogeological appraisal (August 1983to May 1985).Rep. Tabuk Agric. Dev. Co., Tabuk, 58 pp.

Fleitmann, D., Burns, S.J., Neff, U., Mangini, A., Matter, A., 2003. Changing moisture sources over the last 330,000 years in Northern Oman from fluid-inclusion evidence in speleothems. Quaternary Research 60, 223-232.

Fleitmann, D., Matter, A. 2009. The speleothem record of climate variability in Southern Arabia. Geoscience 341: 633–642.

Fleitmann, D., Burns, S.J., Pekala, M., Mangini, A., Al-Subbary, A., Al-Aowah, M., Kramers, J., Matter, A., 2011. Holocene and Pleistocene pluvial periods in Yemen, southern Arabia. Quaternary Science Reviews 30, 783-787.

Garrard, A.N., Harvey, C.P.D., Switsur, V.R., 1981. Environment and settlement during the Upper Pleistocene and Holocene at Jubba in the Great Nefud, northern Arabia. ATLAL - Journal of Saudi Arabian Archaeology 5, 137-148.

Garzanti, E., Vermeesch, P., Andò, S., Vezzoli, G., Valagussa, M., Allen, K., Kadi, K.A., Al-Juboury, A.I.A., 2013. Provenance and recycling of Arabian desert sand. Earth-Science Rev. 120, 1–19. doi:10.1016/j.earscirev.2013.01.005

Ginau, A., Engel, M., & Brückner, H., 2012. Holocene chemical precipitates in the continental sabkha of Tayma (NW Saudi Arabia). Journal of Arid Environments 84, 26-37.

Green, R.E., Krause, J., Briggs, A.W., Maricic, T., Stenzel, U., Kircher, M., Patterson, N., Li, H., Zhai, W., Fritz, M.H.Y. and Hansen, N.F., 2010. A draft sequence of the Neandertal genome. Science, 328(5979), 710-722.

Groucutt, H. S., Petraglia, M. D., Bailey, G., Scerri, E. M. L., Parton, A., Clark-Balzan, L., Jennings, R. P., Lewis, L., Blinkhorn, J., Drake, N. A., Breeze, P. S., Inglis, R. H., Devès, M. H., Meredith-Williams, M., Boivin, N., Thomas, M. G., Scally, A. 2015a. Rethinking the dispersal of Homo sapiens out of Africa. Evolutionary Anthropology: Issues, News, and Reviews, 24(4), 149–164. http://doi.org/10.1002/evan.21455

Groucutt, H.S., White, T.S., Clark-Balzan, L., Parton, A., Crassard, R., Shipton, C., Jennings, R.P., Parker, A.G., Breeze, P.S., Scerri, E.M.L., Alsharekh, A., Petraglia, M.D., 2015b. Human occupation of the Arabian Empty Quarter during MIS 5: Evidence from Mundafan Al-Buhayrah, Saudi Arabia. Quaternary Science Reviews. 119, 116–135. doi:10.1016/j.quascirev.2015.04.020

Groucutt, H. S., E. M. L. Scerri., L. Lewis, L. Clark-Balzan, J. Blinkhorn, R. P. Jennings, A. Parton, and M. D. Petraglia. 2015c. Stone tool assemblages and models for the dispersal of Homo sapiens out of Africa. Quaternary International 382, 8–30. doi.org/10.1016/j.quaint.2015.01.039

Groucutt, H. S., Scerri, E. M. L., Amor, K., Shipton, C., Jennings, R. P., Parton, A., Clark-Balzan, L., Alsharekh, A., Petraglia, M. D., 2017. Middle Palaeolithic raw material procurement and early stage reduction at Jubbah, Saudi Arabia. Archaeological Research in Asia, 9, 44–62. doi.org/10.1016/j.ara.2017.01.003

Grove, M., 2012. Amplitudes of orbitally induced climatic cycles and patterns of hominin speciation. Journal of Archaeological Science, 39(10), 3085–3094. doi.org/10.1016/j.jas.2012.04.023

Guagnin, M., Jennings, R.P., Clark-Balzan, L., Groucutt, H.S., Parton, A. and Petraglia, M.D., 2015. Hunters and herders: Exploring the Neolithic transition in the rock art of Shuwaymis, Saudi Arabia. Archaeological Research in Asia, 4, 3-16.

Guagnin, M., Jennings, R., Eager, H., Parton, A., Stimpson, C., Stepanek, C., Pfeiffer, M., Groucutt, H.S., Drake, N.A., Alsharekh, A. and Petraglia, M.D., 2016. Rock art imagery as a proxy for Holocene environmental change: A view from Shuwaymis, NW Saudi Arabia. The Holocene, 26(11), 1822-1834.

Guérin, G., Mercier, N., Adamiec, G., 2011. Dose-rate conversion factors: Update. Anc. TL 29, 5–8.

Hamilton, P., 2010. Brachysira brebissonii. In: Diatoms of the United States. http://westerndiatoms.colorado.edu/taxa/species/brachysira_brebissonii

Heiri, O., Lotter, A.F. and Lemcke, G., 2001. Loss on ignition as a method for estimating organic and carbonate content in sediments: reproducibility and comparability of results. Journal of paleolimnology, 25(1), 101-110.

Herold, M., Lohmann, G., 2009. Eemian tropical and subtropical African moisture transport: an isotope modelling study. Climate Dynamics 33, 1075-1088.

Hilbert, Y.H., White, T.S., Parton, A., Clark-Balzan, L., Crassard, R., Groucutt, H.S., Jennings, R.P., Breeze, P., Parker, A., Shipton, C., Al-Omari, A., Alsharekh, A.M., Petraglia, M.D., 2014. Epipalaeolithic occupation and palaeoenvironments of the southern Nefud desert, Saudi Arabia, during the Terminal Pleistocene and Early Holocene. J. Archaeol. Sci. 50, 460–474. doi:10.1016/j.jas.2014.07.023

Hoffmann, G., Rupprechter, M., & Rahn, M., Preusser, F., 2015. Fluvio-lacustrine deposits reveal precipitation pattern in SE Arabia during early MIS 3. Quaternary International 382, 145-153

Huntley, D.J., Lamothe, M., 2001. Ubiquity of anomalous fading in K-feldspars and the measurement and correction for it in optical dating. Can. J. Earth Sci. 38, 1093–1106. doi:10.1139/e01-013

Hussein, M.T., Bazuhair, A.G. and Ageeb, A.E., 1992. Hydrogeology of the Saq formation east of Hail, northern Saudi Arabia. Quarterly Journal of Engineering Geology and Hydrogeology, 25(1), 57-64.

Jennings, R., Parton, A., Groucutt, H., Clark-Balzan, L., Breeze, P., Drake, N. A., Alsharekh, A., Petraglia, M. D. 2014. High-resolution geospatial surveying techniques provide new insights into rock-art landscapes at Shuwaymis, Saudi Arabia. Arabian Archaeology and Epigraphy, 25, 1–21.

Jennings, R.P., Singarayer, J., Stone, E.J., Krebs-Kanzow, U., Khon, V., Nisancioglu, K.H., Pfeiffer, M., Zhang, X., Parker, A., Parton, A., Groucutt, H.S., White, T.S., Drake, N.A., Petraglia, M.D., 2015. The greening of Arabia: multiple opportunities for human occupation of the Arabian Peninsula during the Late Pleistocene inferred from an ensemble of climate model simulations. Quat. Int. 382, 181-199. doi.org/10.1016/j.quaint.2015.01.006.

Jennings, R. P., Parton, A., Clark-Balzan, L., White, T. S., Groucutt, H. S., Breeze, P. S., Parker, A. G., Drake, N. A., Petraglia, M. D., 2016. Human occupation of the northern Arabian interior during early Marine Isotope Stage 3. Journal of Quaternary Science, 31(8), 953–966. doi.org/10.1002/jqs.2920

Kaufman, A., Ghaleb, B., Wehmiller, J.F., Hillaire-Marcel, C., 1996. Uranium concentration and isotope ratio profiles within Mercenaria shells: Geochronological implications. Geochim. Cosmochim. Acta 60, 3735–3746. doi:10.1016/0016-7037(96)00190-1

Krammer, K. and Lange-Bertalot, H., 1986. Bacillariophyceae 1. Teil Naviculaceae. Stuttgart, Gustav Fisher Verlag.

Krammer, K. and Lange-Bertalot, H., 1988. Bacillariophyceae 2. Teil Epithemiaceae, Surirellaceae. Stuttgart, Gustav Fisher Verlag

Krammer, K. and Lange-Bertalot, H., 1991a. Bacillariophyceae 3. Teil Centrales, Fragilariaceae, Eunotiaceae. Stuttgart, Gustav Fisher Verlag

Krammer, K. and Lange-Bertalot, H., 1991b. Bacillariophyceae 4. Teil Achnanthaceae, Kritishe Ergänzungen zu Navicula (Lineolate) und Gomphonema. Stuttgart, Gustav Fisher Verlag

Krbetschek, M.R., Rieser, U., Zöller, L., Heinicke, J., 1994. Radioactive disequilibria in palaeodosimetric dating of sediments. Radiat. Meas. 23, 485–489.

Lamb, A.L., Leng, M.J., Lamb, H.F., Mohammed, M.U., 2000. A 9000-year oxygen and carbon isotope record of hydrological change in a small Ethiopian crater lake. The Holocene 10, 167-177.

Larrasoaña, J. C., Roberts, A. P., Rohling, E. J., Winklhofer, M., and Wehausen, R. (2003). Three million years of monsoon variability over the northern Sahara. Climate Dynamics 21, 689–698.

Legezynska, E., Wiktor, K., 1981. Bottom fauna of the Inner Puck Bay. Zesz. Nauk. UG, Oceanografia, 8, 63-77.

Leng, M.J. and Marshall, J.D., 2004. Palaeoclimate interpretation of stable isotope data from lake sediment archives. Quaternary Science Reviews, 23(7), 811-831.

Lloyd, J.W. and Pim, R.H., 1990. The hydrogeology and groundwater resources development of the Cambro-Ordovician sandstone aquifer in Saudi Arabia and Jordan. Journal of Hydrology, 121(1-4), 1-20.

Marty, J., Myrbo, A., 2014. Radiocarbon dating suitability of aquatic plant macrofossils. J. Paleolimnol. 52: 435-443. doi:10.1007/s10933-014-9796-0

Maslin, M. A., Brierley, C. M., Milner, A. M., Shultz, S., Trauth, M. H., Wilson, K. E. 2014. East African climate pulses and early human evolution. Quaternary Science Reviews. 301, 1-17. doi.org/10.1016/j.quascirev.2014.06.012

Matter, A., Neubert, E., Preusser, F., Rosenberg, T., Al-Wagdani, K., 2015. Palaeo-environmental implications derived from lake and sabkha deposits of the southern Rub' al-Khali, Saudi Arabia and Oman. Quat. Int. 382, 120–131.

Matter, A., Mahjoub, A., Neubert, E., Preusser, F., Schwalb, A., Szidat, S., Wulf, G., 2016. Reactivation of the Pleistocene trans-Arabian Wadi ad Dawasir fluvial system (Saudi Arabia) during the Holocene humid phase. Geomorphology 270, 88–101.

McClure, H.A., 1976. Radiocarbon chronology of late Quaternary lakes in the Arabian desert. Nature 263, 755.

Meyers, D., 2014. Epithemia argus. In: Diatoms of the United States. http://westerndiatoms.colorado.edu/taxa/species/epithemia_argus

Morellón, M., Valero-Garcés, B., Moreno, A., González-Sampériz, P., Mata, P., Romero, O., Maestro, M. and Navas, A., 2008. Holocene palaeohydrology and climate variability in northeastern Spain: the sedimentary record of Lake Estanya (Pre-Pyrenean range). Quaternary International, 181(1), 15-31.

Murray, A.S., Wintle, A.G., 2000. Luminescence dating of quartz using an improved single-aliquot regenerative-dose protocol. Radiat. Meas. 32, 57–73. doi:10.1016/S1350-4487(99)00253-X

Murray, A.S., Wintle, A.G., 2003. The single aliquot regenerative dose protocol: Potential for improvements in reliability. Radiat. Meas. 37, 377–381. doi:10.1016/S1350-4487(03)00053-2

Nakov, T., Guillory, W., Julius, M., Theriot, E. and Alverson, A., 2015. Towards a phylogenetic classification of species belonging to the diatom genus Cyclotella (Bacillariophyceae): Transfer of species formerly placed in Puncticulata, Handmannia, Pliocaenicus and Cyclotella to the genus Lindavia. Phytotaxa, 217(3), 249-264.

Nathan, R.P., Mauz, B., 2008. On the dose-rate estimate of carbonate-rich sediments for trapped charge dating. Radiat. Meas. 43, 14–25. doi:10.1016/j.radmeas.2007.12.012

Nathan, R.P., Thomas, P.J., Jain, M., Murray, a. S., Rhodes, E.J., 2003. Environmental dose rate heterogeneity of beta radiation and its implications for luminescence dating: Monte Carlo modelling and experimental validation. Radiat. Meas. 37, 305–313. doi:10.1016/S1350-4487(03)00008-8

Olley, J.M., Murray, A., Roberts, R.G., 1996. The effects of disequilibria in the uranium and thorium decay chains on burial dose rates in fluvial sediments. Quat. Sci. Rev. 15, 751-760.

Oswald, W.W., Anderson, P.M., Brown, T.A., Brubaker, L.B., Hu, F.S., Lozhkin, A. V, Tinner, W., Kaltenrieder, P., 2005. Effects of sample mass and macrofossil type on radiocarbon dating of arctic and boreal lake sediments. The Holocene 15, 758–767.

Parker, A.G., Eckersley, L., Smith, M.M., Goudie, A.S., Stokes, S., White, K., Hodson, M.J., 2004. Holocene vegetation dynamics in the northeastern Rub' al-Khali desert, Arabian Peninsula: a pollen, phytolith and carbon isotope study. Journal of Quaternary Science 19, 665–676.

Parker, A.G., Goudie, A.S., Stokes, S., White, K., Hodson, M.J., Manning, M., Kennet, D., 2006. A record of Holocene climate change from lake geochemical analyses in south-eastern Arabia. Quat. Res. 66, 465–476.

Parker, A. G., Preston, G. W., Parton, A., Walkington, H., Jardine, P. E., Leng, M. J., & Hodson, M. J., 2016. Low-latitude Holocene hydroclimate derived from lake sediment flux and geochemistry. Journal of Quaternary Science, 31(4), 286–299. doi.org/10.1002/jqs.2859

Parton, A., Farrant, A.R., Leng, M.J., Schwenninger, J.-L., Rose, J.I., Uerpmann, H.-P., Parker, A.G., 2013. An early MIS 3 pluvial phase in Southeast Arabia: climatic and archaeological implications. Quaternary International 300, 62-74.

Parton, A., Farrant, A.R., Lang, M.J., Telfer, M.W., Groucutt, H.S., Petraglia, M.D., Parker, A.G., 2015a. Alluvial fan records from southeast Arabia reveal multiple windows for human dispersal. Geology 43 (4), 295-298. doi.org/ 10.1130/g36401.1.

Parton, A., White, T.S., Parker, A., Breeze, P.S., Jennings, R., Groucutt, H.S., Petraglia, M.D., 2015b. Orbital-scale climate variability in Arabia as a potential motor for human dispersals. Quat. Int. 382, 82e97. doi.org/10.1016/ j.quaint.2015.01.005.

Petraglia, M.D., Alsharekh, A.M., Crassard, R., Drake, N.A., Groucutt, H., Parker, A.G., Roberts, R.G., 2011. Middle Paleolithic occupation on a Marine Isotope Stage 5 lakeshore in the Nafud Desert, Saudi Arabia. Quaternary Science Reviews 30, 1555-1559.

Petraglia, M.D., Alsharekh, A., Breeze, P., Clarkson, C., Crassard, R., Drake, N.A., Groucutt, H.S., Jennings, R., Parker, A.G., Parton, A., Roberts, R.G., Shipton, C., Matheson, C., al-Omari, A., Veall, M. A., 2012. Hominin dispersal into the Nefud desert and Middle Palaeolithic settlement along the Jubbah palaeolake, northern Arabia. PLoS ONE 7, e49840.

Poulíčková, A. and Jahn, R., 2007. Campylodiscus clypeus (Ehrenberg) Ehrenberg ex Kützing: Typification, morphology and distribution. Diatom Research, 22(1), 135-146.

Preston, G.W., Thomas, D.S.G., Goudie, A.S., Atkinson, O.A.C., Leng, M.J., Hodson, M.J., Walkington, H., Charpentier, V., Méry, S., Borgi, F., Parker, A.G., 2015. A multi-proxy analysis of the Holocene humid phase from the United Arab Emirates and its implications for southeast Arabia's Neolithic populations. Quat. Int. 382, 277–292.

Preusser, F., Radies, D., Matter, A., 2002. A 160,000 year record of dune development and atmospheric circulation in Southern Arabia. Science 296, 2018-2020.

Radies, D., Hasiotis, S.T., Preusser, F., Neubert, E., Matter, A., 2005. Paleoclimatic significance of Early Holocene faunal assemblages in wet interdune deposits of the Wahiba Sand Sea, Sultanate of Oman. J. Arid Environ. 62, 109–125.

Reimer, P.J., Bard, E., Bayliss, A., Beck, J.W., Blackwell, P.G., Bronk Ramsey, C., Buck, C.E., Cheng, H., Edwards, R.L., Friedrich, M., Grootes, P.M., Guilderson, T.P., Haflidason, H., Hajdas, I., Hatté, C., Heaton, T.J., Hoffmann, D.L., Hogg, A.G., Hughen, K.A., Kaiser, K.F., Kromer, B., Manning, S.W., Niu, M., Reimer, R.W., Richards, D.A., Scott, E.M., Southon, J.R., Staff, R.A., Turney, C.S.M., van der Plicht, J., 2013. IntCal13 and Marine13 Radiocarbon Age Calibration Curves 0-50,000 Years cal BP. Radiocarbon 55, 1869–1887. doi:10.2458/azu_js_rc.55.16947

Renberg, I., 1990. A procedure for preparing large sets of diatom slides from sediment cores. Journal of Paleolimnology, 4(1), 87-90.

Revel, M.E., Ducassou, E., Grousset, F.E., Bernasconi, S.M., Migeon, S., Revillon, S., Mascle, J., Murat, A., Zaragosi, S., Bosch, D,. 2010. 100,000 years of African monsoon variability recorded in sediments of the Nile margin. Quaternary Science Reviews 29, 1342–1362

Rosenberg, T.M., Preusser, F., Fleitmann, D., Schwalb, A., Penkman, K., Schmid, T.W., Al-Shanti, M.A., Kadi, K., Matter, A., 2011a. Humid periods in southern Arabia: Windows of opportunity for modern human dispersal. Geology 39, 1115–1118. doi:10.1130/G32281.1

Rosenberg, T.M., Preusser, F., Wintle, A.G., 2011b. A comparison of single and multiple aliquot TT-OSL data sets for sand-sized quartz from the Arabian Peninsula. Radiat. Meas. 46, 573–579. doi:10.1016/j.radmeas.2011.03.020

Rosenberg, T.M., Preusser, F., Risberg, J., Plikk, A., Kadi, K.K., Matter, A., Fleitmann, D., 2013. Middle and Late Pleistocene humid periods recorded in palaeolake deposits of the Nafud desert, Saudi Arabia. Quaternary Science Reviews 70, 109-123.

Saros, J. E. and Anderson, N. J., 2014. The ecology of the planktonic diatom Cyclotella and its implications for global environmental change studies. Biological Reviews. doi: 10.1111/brv.12120

Scerri, E. M. L., S. P. Breeze, A. Parton, H. S. Groucutt, T. S. White, C. Stimpson, L. Clark-Balzan, R. Jennings, A. Alsharekh, and M. D. Petraglia. 2015. Middle to Late Pleistocene Human Habitation in the Western Nefud Desert, Saudi Arabia. Quaternary International 382, 200–214.

Shea, J. J., 2008. Transitions or turnovers? Climatically-forced extinctions of Homo sapiens and Neanderthals in the east Mediterranean Levant. Quaternary Science Reviews, 27(23-24), 2253–2270. doi.org/doi:10.1016/j.quascirev.2008.08.015

Shipton, C., Parton, A., Breeze, P., Jennings, R., Groucutt, H.S., White, T.S., Drake, N., Crassard, R., Alsharekh, A., Petraglia, M.D., 2014. Large Flake Acheulean in the Nefud Desert of northern Arabia. Paleoanthropology 2014, 446-462.

Spaulding, S., and Metzeltin, D., 2011. *Rhopalodia*. In Diatoms of the United States. http://westerndiatoms.colorado.edu/taxa/genus/rhopalodia

Staubwasser, M., & Weiss, H., 2006. Holocene climate and cultural evolution in late prehistoric–early historic West Asia. Quaternary Research, 66(3), 372–387.

Stimpson, C.M., Lister, A., Parton, A., Clark-Balzan, L., Breeze, P.S., Drake, N.A., Groucutt, H.S., Jennings, R., Scerri, E.M., White, T.S., Zahir, M., 2016. Middle Pleistocene vertebrate fossils from the Nefud Desert, Saudi Arabia: implications for biogeography and palaeoecology. Quaternary Science Reviews, 143, 13-36.

Ter Braak, C.J. and Prentice, I.C., 1988. A theory of gradient analysis. Advances in ecological research, 18, 271-317.

Thatcher, L., Rubin, M., Brown, G.F., 1961. Dating Desert Ground Water. Science (3472). 134, 105–106.

Thiel, C., Buylaert, J.P., Murray, A., Terhorst, B., Hofer, I., Tsukamoto, S., Frechen, M., 2011a. Luminescence dating of the Stratzing loess profile (Austria)—Testing the potential of an elevated temperature post-IR IRSL protocol. Quat. Int. 234, 23–31. doi:10.1016/j.quaint.2010.05.018

Thiel, C., Buylaert, J.-P., Murray, A.S., Tsukamoto, S., 2011b. On the applicability of post-IR IRSL dating to Japanese loess. Geochronometria 38, 369–378. doi:10.2478/s13386-011-0043-4

Trauth, M. H., Deino, A. L., Bergner, A. G. N., & Strecker, M. R., 2003. East African climate change and orbital forcing during the last 175 kyr BP. Earth and Planetary Science Letters, 206(3-4), 297–313. doi.org/10.1016/S0012-821X(02)01105-6

Trauth, M. H., Maslin, M. A., Deino, A. L., Strecker, M. R., Bergner, A. G. N., & Dühnforth, M., 2007. High- and low-latitude forcing of Plio-Pleistocene East African climate and human evolution. Journal of Human Evolution, 53(5), 475–486. doi.org/10.1016/j.jhevol.2006.12.009

Trommer, G., Siccha, M., Rohling, E.J., Grant, K., van der Meer, M.T.J., Schouten, S., Baranowski, U., Kucera, M., 2011. Sensitivity of Red Sea circulation to sea level and insolation forcing during the last interglacial. Climate of the Past 7, 941-955.

UN-ESCWA and BGR (United Nations Economic and Social Commission for Western Asia; Bundesanstalt für Geowissenschaften und Rohstoffe). 2013. Inventory of Shared Water Resources in Western Asia. Beirut.

Vaks, A., Bar-Matthews, M., Matthews, A., Ayalon, A., Frumkin, A., 2010. Middle-Late Quaternary paleoclimate of northern margins of the Saharan-Arabian Desert: reconstruction from speleothems of Negev Desert, Israel. Quaternary Science Reviews 29, 2647-2662.

Vincent, P., 2008. Saudi Arabia An Environmental Overview, London, Taylor & Francis Group

Wagner, W., 2011. Groundwater in the Arab Middle East. Springer Science & Business Media.

Waldmann, N., Torfstein, A., Stein, M., 2010. Northward intrusions of low- and mid-latitude storms across the Saharo-Arabian belt during past interglacials. Geology 38 (6), 567-570.

Whitney, J.W., Gettings, M.E., 1982. Preliminary Geological Investigation of the Bir Hayzan Diatomite Deposit, Kingdom of Saudi Arabia. USGS Open-File Report - OF-02-7. Saudi Arabian Deputy Ministry for Mineral Resources, Riyadh.

Whitney, J.W., Faulkender, D.J., Rubin, M., 1983. The Environmental History and Present Condition of Saudi Arabia's Northern Sand Seas. USGS Open-File Report. Saudi Arabian Deputy Ministry for Mineral Resources, Riyadh.

Williams, M.A.J., Duller, G.A.T., Williams, F.M., Woodward, C.J., Macklin, M.G., El Tom, O.A.M., Munro, R.N., El Hajaz, Y., Barrows, T.T., 2015. Causal links between Nile floods and eastern Mediterranean sapropel formation during the past 125 kyr confirmed by OSL and radiocarbon dating of Blue and White Nile sediments. Quaternary Science Reviews 130, 89–108

Wood, W.W. and Osterkamp, W.R., 1987. Playa-lake basins on the Southern High Plains of Texas and New Mexico: Part II. A hydrologic model and mass-balance arguments for their development. Geological Society of America Bulletin, 99(2), 224-230.

Wood, W.W., Rizk, Z.S., Alsharhan, A.S., 2003. Timing of recharge, and the origin, evolution, and distribution of solutes in a hyperarid aquifer system. In: Alsharhan, A.S., Wood, W.W. (Eds.), Water Resources Perspectives: Evaluation Management and Policy. Elsevier, Amsterdam, pp. 295-312.